MODELING THE IMPACTS OF A DIRECTLY LANDFALLING TROPICAL CYCLONE ON

**COASTAL GEORGIA** 

by

**KYLE BROOKS** 

(Under the Direction of John A. Knox)

**ABSTRACT** 

Tropical cyclones (TCs) are one of the deadliest and costliest natural disasters in the United

States and worldwide. The Georgia Coastline has not been directly impacted by a landfalling TC

since October 1898. The "1898 Georgia Hurricane" was an intense TC that caused catastrophic

flooding in SE Georgia and NE Florida. This study uses WRF-ARW to downscale reanalysis data

from the NOAA/DOE 20th Century Reanalysis version 3 dataset. Climate data was then used to

analyze the storm as it would progress in 1898, 2024, and 2098 climate conditions. Results indicate

that the 1898 storm might have been weaker than it is recorded in the HURDAT2 database, but

the modeled surge was still catastrophic. Warmer climate conditions also failed to produce a more

intense TC regardless of the intensity metric. Furthermore, a major hurricane may not be necessary

to produce the surge recorded in observations.

INDEX WORDS:

Tropical cyclones, Numerical weather prediction, Reanalysis, Storm

surge, WRF-ARW, Georgia coast

# MODELING THE IMPACTS OF A DIRECTLY LANDFALLING TROPICAL CYCLONE ON COASTAL GEORGIA

by

## **KYLE BROOKS**

B.S, University of Georgia, 2022

A Thesis Submitted to the Graduate Faculty of The University of Georgia in Partial Fulfillment of the Requirements for the Degree

MASTER OF SCIENCE

ATHENS, GEORGIA

2025

© 2025

Kyle Brooks

All Rights Reserved

# MODELING THE IMPACTS OF A DIRECTLY LANDFALLING TROPICAL CYCLONE ON ${\sf COASTAL\ GEORGIA}$

by

## **KYLE BROOKS**

Major Professor: John A. Knox

Committee: J. Marshall Shepherd

Gabriel J. Kooperman

Electronic Version Approved:

Ron Walcott Vice Provost for Graduate Education and Dean of the Graduate School The University of Georgia May 2025

# **DEDICATION**

Keelan, Noah, Mandy, Jada, Alvin, Mom, Dad, and Volta: thank you for reminding me to never stop chasing.

## **ACKNOWLEDGEMENTS**

This study was conducted with high-performance computing support from the Derecho supercomputer (doi.10.5065/qx9a-pg09) supported by NSF's National Centers for Atmospheric Research (NCAR) at the NSF NCAR-Wyoming Supercomputing Center, sponsored by the National Science Foundation and the State of Wyoming. We would also like to acknowledge computing support for data analysis from the Casper system (<a href="https://ncar.pub/casper">https://ncar.pub/casper</a>) provided by the NSF National Center for Atmospheric Research (NCAR), sponsored by the National Science Foundation.

## TABLE OF CONTENTS

	Page
DEDICATION	iv
ACKNOWLEDGEMENTS	V
LIST OF TABLES	viii
LIST OF FIGURES	ix
CHAPTER	
1 Introduction	1
Research Questions and Objectives	3
2 Background	4
Coastal Georgia's Hurricane History	4
Georgia's Societal Vulnerabilities to Tropical Cyclor	nes6
Tropical Cyclones and Climate Change	9
The 1898 TC in IBTRaCS (HURDAT2)	12
Summary	13
3 Methodology	14
Case Selection and Data Sources	14
The WRF-ARW Model	15
Model Parameterizations and Physics	15
Model Domains	17
Initializing WRF with 20CRv3	18
Spectral Nudging	19
Stochastic Kinetic-Energy Backscatter Scheme	20

	Pseudo Global Warming	21
	The Sea Lake and Overland Surges from Hurricanes (SLOSH) Model	23
4	Results	24
	Modeling of the Storm: October 1-4, 1898	24
	SSP 370: 1898 TC in Present-day Climate Conditions (2024)	35
	SSP 370: 1898 TC in Future Climate Conditions (2098)	42
5	Discussion	50
	Modeled 1898 TC vs. Observed TC	50
	Potential Effects of a Similar Storm Today (2025)	53
	Some Impacts of Future Climate Forcing on the 1898 TC	54
	Important Considerations for this Modeling Study	55
	Lack of Certainty in Surface Wind Speeds	56
6	Conclusions and Future Work	58
REFERE	NCES	60

# LIST OF TABLES

Page
Table 1: List of all landfalling south-east Atlantic Coast TCs (1851-2004)5
Table 2: Archeological sites in coastal Georgia under threat from different magnitudes of sea-
level rise (from Howland and Thompson 2024)16
Table 3: WRF-ARW parameterization settings used for this study

## LIST OF FIGURES

Pa	age
Figure 1: Spatial distribution of Georgia TC landfalls	5
Figure 2: Destruction in Mexico Beach, FL shortly after Hurricane Michael (2018)	7
Figure 3: A map of Georgia showing interstates. I-16 is circled in red	7
Figure 4: Satellite imagery of Tybee Island, GA showing U.S 80	9
Figure 5: Imagery of a tidal march along U.S 80 west of Tybee Island	.10
Figure 6: Imagery of U.S 80 bridge just west of Tybee Island, GA	.10
Figure 7: NOAA storm surge risk maps for the southeast Atlantic Coast for a category 1 (left)	
and category 2 (right) storm	.11
Figure 8: TC return periods (from Keim et al. 2007)	.12
Figure 9: Raw data for the 1898 TC from HURDAT2	.13
Figure 10: IBTRaCS visualization of the 1898 TC	.14
Figure 11: D01 (larger) and the vortex-following D02 (smaller) used in this study	.18
Figure 12: 800 mb geopotential height contours from WRF-ARW (A) and 20CRv3 (B). The re-	ed
'X' represents the storm center from WRF-ARW	.25
Figure 13: 1898 TC tracks from HURDAT2, 20CRv3, and WRF-ARW	.26
Figure 14: Tracks of the modeled mean 1898 TC and ensemble members	.26
Figure 15: The 1898 TC's mean forward speed	.27
Figure 16: 1898 TC modeled MSLP (15-minute average)	.28
Figure 17: 1898 TC modeled maximum wind speed (15-minute average)	.29

Figure 18: 1898 TC modeled wind field at landfall	29
Figure 19: 1898 TC run-total (~ 60 hours) modeled accumulated precipitation	30
Figure 20: 1898 TC modeled MSLP for 4 select cities on the Georgia coast	31
Figure 21: Coastal Georgia cities with their offshore 10m wind measurement points	32
Figure 22: 1898 Modeled TC 10m wind speeds	33
Figure 23: Overview of the modeled 1898 storm surge	34
Figure 24: Same as figure 23 but zoomed on the Brunswick, GA area	35
Figure 25: Tracks of the modeled mean 2024 TC and ensemble members	36
Figure 26: The 2024 TC's mean forward speed	37
Figure 27: 2024 TC modeled MSLP (15-minute average)	38
Figure 28: 2024 TC modeled maximum wind speed (15-minute average)	39
Figure 29: 2024 TC modeled wind field at landfall	39
Figure 30: 2024 TC run-total (~ 60 hours) modeled accumulated precipitation	40
Figure 31: 2024 TC modeled MSLP for 4 select cities on the Georgia coast	40
Figure 32: 1898 Modeled TC 10m wind speeds for 4 select cities on the Georgia coast	41
Figure 33: Overview of the modeled 2024 storm surge	41
Figure 34: Same as Fig. 33 but zoomed in on the Brunswick, GA area	42
Figure 35: Tracks of the modeled mean 2098 TC and ensemble members	43
Figure 36: The 2098 TC's mean forward speed	43
Figure 37: 2098 TC modeled MSLP (15-minute average)	44
Figure 38: 2098 TC modeled maximum wind speed (15-minute average)	44
Figure 39: 2098 TC modeled wind field at landfall	45
Figure 40: 2098 TC run-total (~ 60 hours) modeled accumulated precipitation	46

Figure 41: 2098 TC modeled MSLP for 4 select cities on the Georgia coast
Figure 42: 2098 Modeled TC 10m wind speeds for 4 select cities on the Georgia coast48
Figure 43: Overview of the modeled 2024 storm surge
Figure 44: Same as Fig. 43 but zoomed in on the Savannah, GA area49
Figure 45: Satellite imagery of I-95 crossing the Altamaha River. Developments are seen north
of the river51
Figure 46: An undated picture taken in Brunswick, GA just after the 1898 TC52
Figure 47: Example of 10m windspeed showing a stark contrast between land and ocean,
especially along the northeast Florida coast

#### CHAPTER 1

#### **INTRODUCTION**

Coastal Georgia has not been subjected to the impacts of a directly landfalling tropical cyclone (TC) since 1898. Within this time, the coastal population has increased by 367% from just over 100,000 in 1900 to 555,000 in 2020 (U.S. Census, 1900, 2020). Coastal development occurring with this increase in population has produced a situation with potential for numerous impacts from a major TC making landfall in the area.

The Georgia "Barrier Islands," widely thought to protect the coast from hurricane landfalls, are laden with development patterns that do not logically coincide with the islands' status as protectors from TCs (U.S. Census 2020). Examples of populous developments include towns such as Tybee Island (2020 pop. 3,114) and Census Designated Places such as St. Simons (2020 pop. ~15,000). Furthermore, during the early months of the Atlantic Hurricane Season (June-August), these populations swell as citizens from inland places venture to the beach on vacation to escape the summer heat (City of Tybee Island). During the lull in landfalling TCs over the last 125 years, these communities have prospered. This 'drought' in landfalling storms in coastal Georgia does not mean one may not make landfall in the region to potentially catastrophic effects.

Some cities along the coastline have large populations of adults over the age of 65 and/or people who are living below the poverty line. Almost half (47%) of the population of Tybee Island, GA is over the age of 65 and the average age is ~59 years old (U.S. Census Bureau 2023). However, only 10% of Tybee Island's total population is below the poverty line with 4% of senior citizens living below the line (U.S. Census Bureau 2023). Further north, in Savannah, GA, the population is much younger on average (~34 years old) but has a much higher rate of poverty across all ages with ~20% of the total population below the poverty line. Of senior citizens >65

years old, 20% of them live below the poverty line (U.S. Census Bureau 2023). Further south along the coast, Brunswick, GA, has a young population (avg. ~39 years old), of which ~29% live in poverty, with 24% of senior citizens below the poverty line (U.S. Census Bureau 2023). While this is a high-level overview of demographics in select cities along the Georgia Coast, there is evidence of populations that are vulnerable, whether it be from age or because they live in poverty.

Using numerical weather models via the National Centers for Atmospheric Research (NCAR) Advanced Research Weather Research and Forecasting model (WRF-ARW) along with 19<sup>th</sup> century reanalysis data, this study aims to recreate the impacts of the last major landfalling TC from 1898 on a modern Georgia coastline. Furthermore, impacts of climate change on the strength of the storm are simulated through perturbations of WRF-ARW by data from the Community Earth Systems Model-Large Ensemble (CESM2-LENS). To simulate the storm at a higher resolution, vortex-following options in WRF-ARW are utilized to track the cyclone as it progresses.

This study seeks to produce a storm like the 1898 Georgia TC and to quantify some of its impacts on the region where it made landfall. Some of these impacts, especially storm surge, could cause unprecedented problems for the populations along the coast of Georgia. As such, a recreation of this storm in WRF-ARW while using storm surge modeling through the Sea Lake and Overland Surges from Hurricanes (SLOSH) model from NOAA could yield potentially beneficial results for government agencies, planning, and emergency management along coastal Georgia. While many storms have been reanalyzed using models for verification purposes (i.e., Sandrik 1998), the author is not aware of any studies downscaling this type of event using the WRF-ARW. Therefore, this study will be novel as it is the first to model a 19<sup>th</sup> century TC using WRF and 20<sup>th</sup> Century Reanalysis version 3 (20CRv3).

# **Research Questions and Objectives**

- 1: How would a TC like the 1898 storm affect the coastline of Georgia today?
- 2: To what spatial extent would damage from a TC like the one from 1898 occur?
- 3: How well does WRF-ARW downscale a 19<sup>th</sup> century TC from the 20<sup>th</sup> Century Reanalysis version 3 dataset?

#### **CHAPTER 2**

#### BACKGROUND

#### **Coastal Georgia's Hurricane History**

A review of coastal Georgia's history of landfalling TCs reveals a sporadic but non-negligible history of landfalls. The most recent major TC to make landfall directly on coastal Georgia was the 1898 Georgia Hurricane. There is disagreement in literature regarding the exact location of the storm's landfall with location ranging from Fernandina Beach, FL to Brunswick, GA (e.g., Sandrik 1998). The storm is estimated to have killed 179 people and maintains the record for storm surge for Georgia with 16 feet recorded in Brunswick (Landsea 2009). While initially thought to have a minimum central pressure of 945 mb, the reanalysis by Sandrik (1998) concluded that the minimum central pressure was around 938 mb along with a radius of maximum winds of 18 nautical miles. These values were determined using NOAA's SLOSH model and inferencing a best fit storm based on storm surge reports from the event (Sandrik and Landsea 2003).

A more comprehensive review conducted by Bossak et al. (2014) indicates some notable trends in TC activity on the Georgia coast. First, temporal patterns followed the large-scale North Atlantic Hurricane Season with activity maxima occurring between August and October. While not statistically significant, there was a slight spatial trend towards the Savannah, Georgia area regarding landfalling TCs (Fig. 1).

Comparisons between Georgia and other Atlantic coastal states, namely North Carolina, South Carolina, and Florida reveal a lack of landfalling TCs. According to NOAA, between 1851 and 2004, Georgia had a total of 20 landfalling TCs with only 3 of these being major TCs. Meanwhile, North Carolina had 46 total TC landfalls (12 major), South Carolina had 31 total TC

landfalls (6 major), and Florida topped the list with 63 landfalling TCs (16 major). Table 1 shows the comparison between these states.

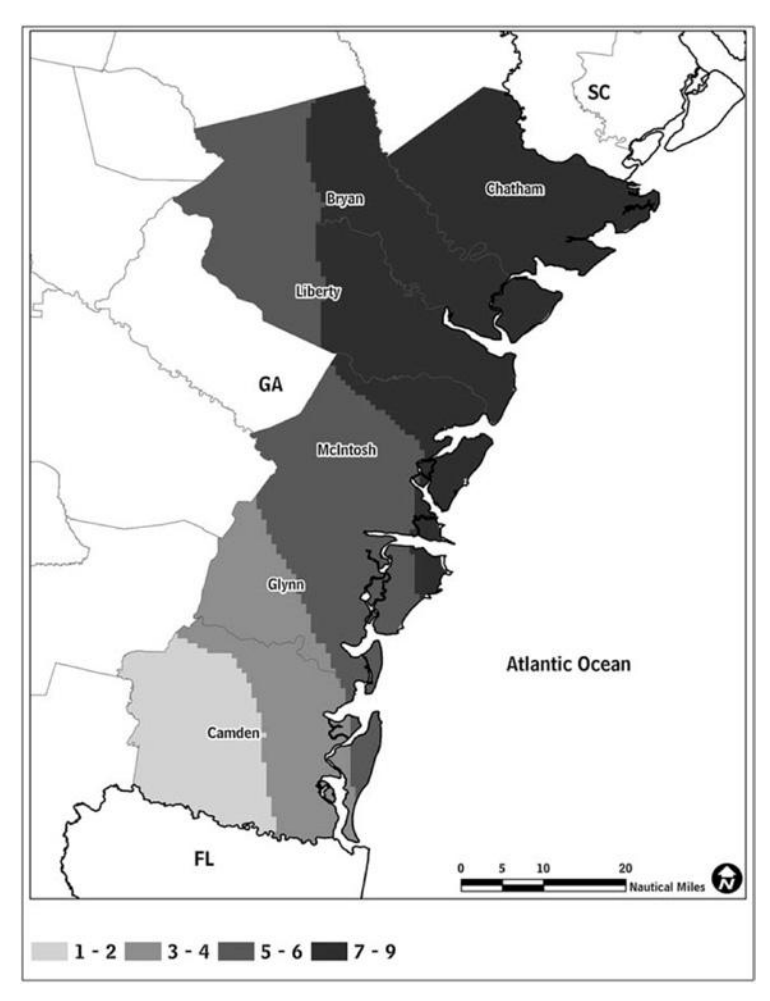


**Figure 1:** Spatial distribution of Georgia TC landfalls (from Bossak et al. 2014)

**Table 1:** List of all landfalling southeast Atlantic Coast TCs (1851-2004)

State	Landfalling TCs (Total)	Landfalling TCs (Major)
Florida (not including Gulf	63	16
coast)		
North Carolina	46	12
South Carolina	31	6
Georgia	20	3

## Georgia's Societal Vulnerabilities to Tropical Cyclones

Agriculture in Georgia contributes approximately \$83.6 billion annually to Georgia's economy (UGA CAES 2022). The growing seasons of key crops in the state coincide with the Atlantic hurricane season which spans from 1 June to 30 November. Georgia leads the nation by far in peanut production with the crop being planted April-June and harvested September-October (USDA 2023). As of 2020, Georgia was the second largest cotton-producing state with most of the crop being planted in the Coastal Plain region (USDA 2020). Outside of crops, forestry is another important industry in Georgia. Native softwood trees are important to Georgia's lumber production. As of 2021, Georgia leads the nation in softwood production and is second only to Alabama in all types of lumber production (Winn et al. 2021). Another staple of Georgia's economy is pecan production in which Georgia is second only to New Mexico (USDA 2024).

In 2018, category 5 Hurricane Michael devastated the coastal plain, especially southwest Georgia, causing more than \$2 billion in losses across all crop sectors (Dowdy 2018; Fig. 2). The 2018 pecan crop alone faced close to \$500 million in losses (Dowdy 2018). Hurricane Michael made landfall in Mexico Beach, Florida as a category 5 and was a category 3 major hurricane when it crossed the Georgia state line. An even more intense storm was Hurricane Helene in 2024 that caused 3 times the damage to Georgia crops and forestry compared to Michael. Hurricane Helene caused an estimated \$6.46 billion in losses (UGA Extension Forsyth County 2024). Despite their effects, Helene and Michael were both indirectly impacting TCs. It is reasonable to assume that a directly impacting TC at similar strength to Hurricane Michael or Helene would cause worse damage with a direct landfall in Georgia. As Michael and Helene were two of the strongest hurricanes to enter modern-day Georgia, they provide some of the few examples of impacts that

could be created by a modern-day Georgia TC. However, Michael and Helene's impacts were inland, and coastal damage in Georgia could not be quantified with either storm.



Figure 2: Destruction in Mexico Beach, FL, shortly after Hurricane Michael (2018)

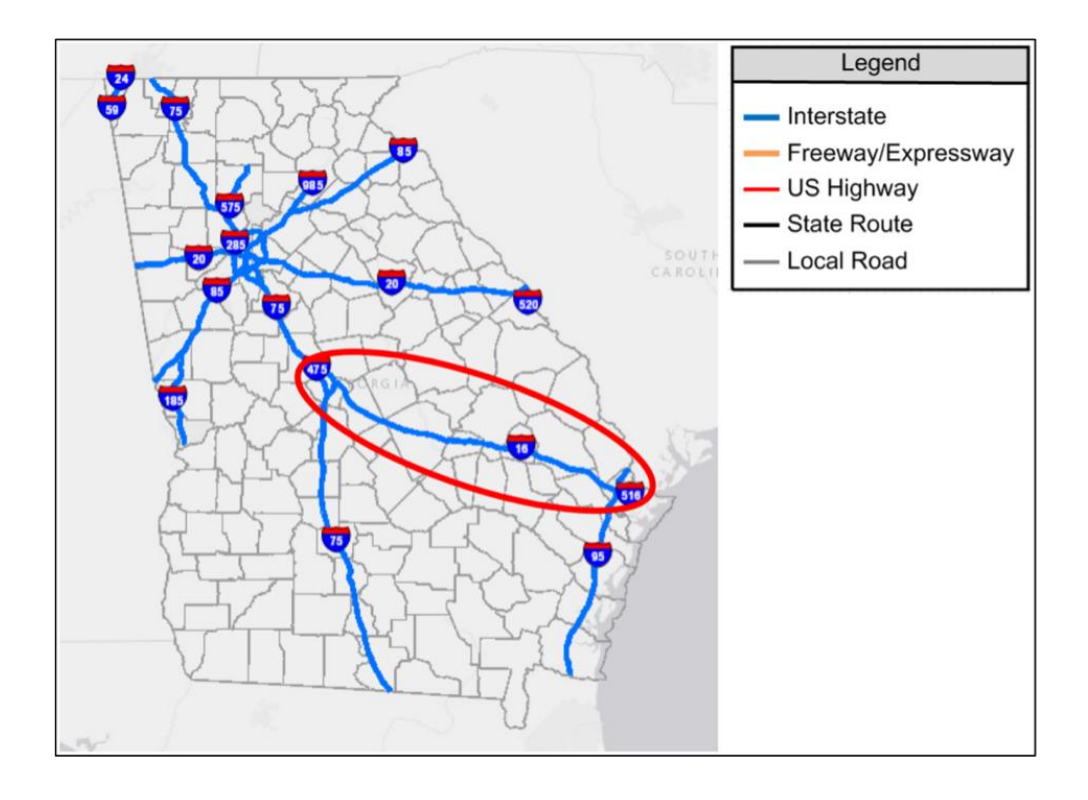


**Figure 3:** A map of Georgia with interstates. I-16 is circled in red

While Georgia's evacuation infrastructure is expansive, there are only 3 major interstates intersecting the coastal plain: I-16 (east-west), I-75 (north-south), and I-95 (north-south) (Fig. 3). An example for potential problems in case of an evacuation of coastal Georgia is I-16. I-16 is of particular importance as it is a designated contraflow highway in times of evacuation with westbound-only traffic between Savannah, Georgia and Dublin, Georgia (GDOT). However, I-16 is the only east-west interstate in Georgia's coastal plain. Hence, it is reasonable to expect potential hazards if the highway becomes impassable because of TC impacts. There is only one real-life example for contraflow traffic on I-16 which occurred when Hurricane Floyd passed close to the Georgia coast without landfall in 1999 (GDOT). There are few resources available regarding the efficacy of the contraflow plan. However, GEMA reports that, in September 1999, Georgia and neighboring states experienced "the largest evacuation effort in American history as Hurricane Floyd bore down on the southeastern coastline" (GEMA 2022).

Some vulnerabilities specific to near-coastline regions can be seen on Google Maps. A prime example is U.S. Highway 80 which, over most of its connecting span between the Tybee Island community and the mainland, has one lane in either direction (Fig. 4). The same roadway also passes through and over several tidal waterways and flood plains that will easily be affected by any storm surge associated with a landfalling TC (Figs. 5, 6). This leaves several communities along the coast in a position ripe for disaster. Landfalling TCs can destroy key bridges and overpasses. A mid-evacuation landfall in this area could be disastrous for life and property. Likewise, U.S. 80 would be crucial to efficient response time by emergency vehicles after a storm. The U.S. National Bridge Inventory includes estimated heights of bridge decks over water surfaces. While several of the bridges in the study area are missing heigh information, the I-95 bridges crossing the Turtle and Little Satilla rivers have deck heights of 35 and 4 feet respectively

(FHA 2024). Further north, near Tybee Island, one U.S. 80 bridge crosses a tributary of the Savannah River at just 6 feet above the water surface (FHA 2024). Official National Hurricane Center Storm Surge Risk Maps show the entirety of the Georgia coast as one of the hotspots for storm surge risk (ArcGIS Dashboard n.d, NOAA 2023, Fig. 7).

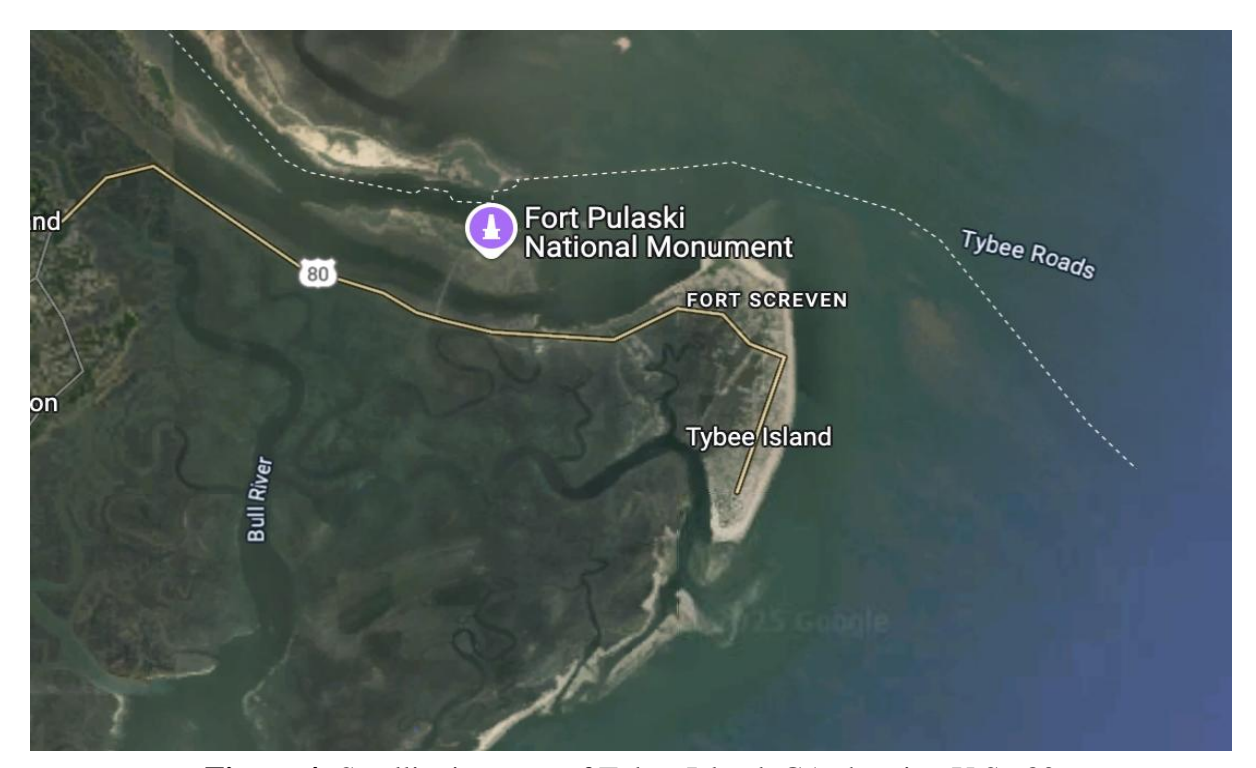


Figure 4: Satellite imagery of Tybee Island, GA showing U.S.. 80

## **Tropical Cyclones and Climate Change**

There is little disagreement among climate scientists that modern climate change is linked to anthropogenic sources. There is more nuance, however, when linking anthropogenic effects on future TC behavior (e.g., Knutson et al. 2020). While a change in the number of TCs in a warmer climate is uncertain, it is believed that a higher proportion of storms will be more intense, with phenomena such as rapid intensification and extreme rainfall becoming more prevalent in a warmer and moister atmosphere (Knutson et al. 2020). The dynamical downscaling of three different climate reanalysis shows an increase in North Atlantic TC (NATC) activity over the last 150 years (Emanuel 2021). However, there is uncertainty regarding the seemingly important

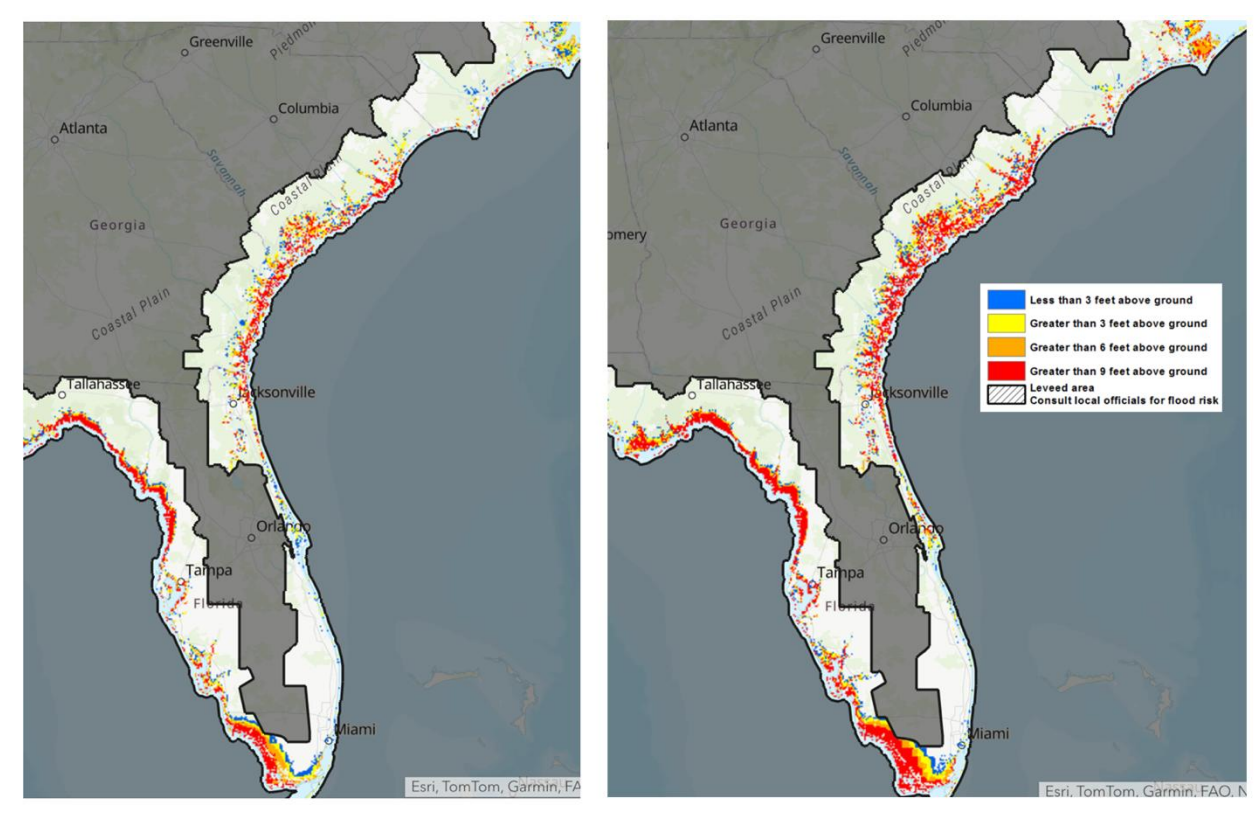
connection between NATCs and climate-driven drought in the Sahel region of Africa indicating the need for more research on this topic (Emanuel 2021).



Figure 5: Imagery of a tidal march along U.S. 80 west of Tybee Island (Google Maps)



Figure 6: Imagery of a U.S. 80 bridge just west of Tybee Island (Google Maps)



**Figure 7:** NOAA storm surge risk maps for the southeast Atlantic Coast for a category 1 (left) and category 2 (right) storm

Additionally, studies show an increasing threat for TC impacts on the Georgia coastline (Keim et al. 2007, Xi et al. 2023, Corkran 2024). Current return periods of landfalling TCs in Georgia range from 52 years on St. Simons Island to 85 years when considering the entire coastline (Keim et al. 2007; Fig. 8 below). These return periods further support the idea of a "TC desert" on the Georgia coast. Furthermore, under high emission scenarios (SSP5 8.5) in climate modeling, the likelihood of sequential tropical cyclone hazards is projected to increase significantly along the Atlantic and Gulf coasts of the United States (Xi et al. 2023). Substantial decreases in the return period of both TCs and sequential hazards are also documented in some studies (Korkran 2024; Xi et al. 2023).

Given the vulnerability of coastal Georgia to storm surge, even with current sea levels, another climate-change induced impact that must be considered is sea-level rise. A 2024 study that

used NOAA's SLOSH model to analyze potential storm surge impacts on archeological sites throughout coastal Georgia indicated a sea level rise of 0.3 meters was enough to drastically increase the threat of storm surge inundation and erosion to coastal archeological sites (Howland and Thompson 2024; Table 2 below). While this study did not look at housing or infrastructure, it may serve as a proxy to indicate that rising sea levels will increase the impact of storm surge from lower-end TCs.

#### The 1898 TC in IBTRaCS (HURDAT2)

HURDAT2, a product of the International Best Track Archive for Climate Stewardship (IBTRaCS, NOAA) has some limited data on the 1898 Georgia TC. When looking at raw text data for the storm only 3 points are available (across all sources) for pressure. The rest of storm intensity metrics (almost entirely windspeeds) are assumed to be estimated (Fig. 9) as their source is only cited as "USA WIND." Given the similarity between HURDAT2 data for the storm and measurements from Sandrik and Landsea (2003), there is the possibility that the best guess storm was taken from this study (Figs. 9, 10). Regardless, the TC made landfall near Brunswick, GA as a category 4 storm with winds of 115 knots around 16 UTC on 2 Oct. 1898 (Fig. 10).

## WRF-ARW for studying TCs

Since the WRF-ARW model is a mesoscale model, there are many examples of WRF-ARW's capacity for studying TCs. A review of selected literature provided confidence that WRF-ARW model could produce an effective TC simulation. Much of the literature using WRF-ARW to study TCs is split into two categories: reanalysis, and model improvement. WRF-ARW has been used to study overland intensification of TCs by reanalyzing TC Erin in 2007 (Evans et al. 2011). Different parameterizations and their effects on TC structure and intensity are also well-researched. One such study from 2009 looked at the effect of WRF-ARW turbulence

parameterizations and grid spacing on an idealized TC simulation (Hill and Lackmann 2009). Furthermore, a 2015 study used WRF-ARW to observe a TC's interaction with the Western Pacific Subtropical High, a large-scale steering mechanism of TCs (Sun et al. 2015).

One aspect of this study, which will be discussed later, is pseudo global warming (PGW). PGW is a method of implementing climate change impacts into datasets like the ones used to initialize WRF in this study. PGW has been used with WRF to research changes in TC characteristics over a 13-year convection permitting model run (Gutmann et al. 2018). More recent studies have used PGW with WRF to study TC intensity and size patterns in future climates in the South China Sea (Chow et al. 2024).

## **Summary**

While coastal Georgia has historically seen fewer tropical cyclone landfalls than surrounding states, the region remains vulnerable to the impacts of a direct landfall. The 1898 Georgia Hurricane continues to serve as the most significant example of what such an event can bring in terms of storm surge and loss of life. Although the storm occurred more than a century ago, limited but focused reanalysis efforts—such as those by Sandrik and Landsea (2003)—have paved the way for more refined reconstructions using modern tools. This work aims to contribute to that foundation by beginning the process of downscaling the 1898 storm using updated modeling techniques. This work underscores the value of integrating historical data with current modeling frameworks as a path toward more accurate risk assessments. As climate change introduces heightened risks through sea-level rise and the potential for stronger, faster-intensifying storms, improving our understanding of past events like the 1898 hurricane will be critical in preparing for future coastal hazards in Georgia. Furthermore, WRF-ARW is an appropriate model to downscale this historical storm.

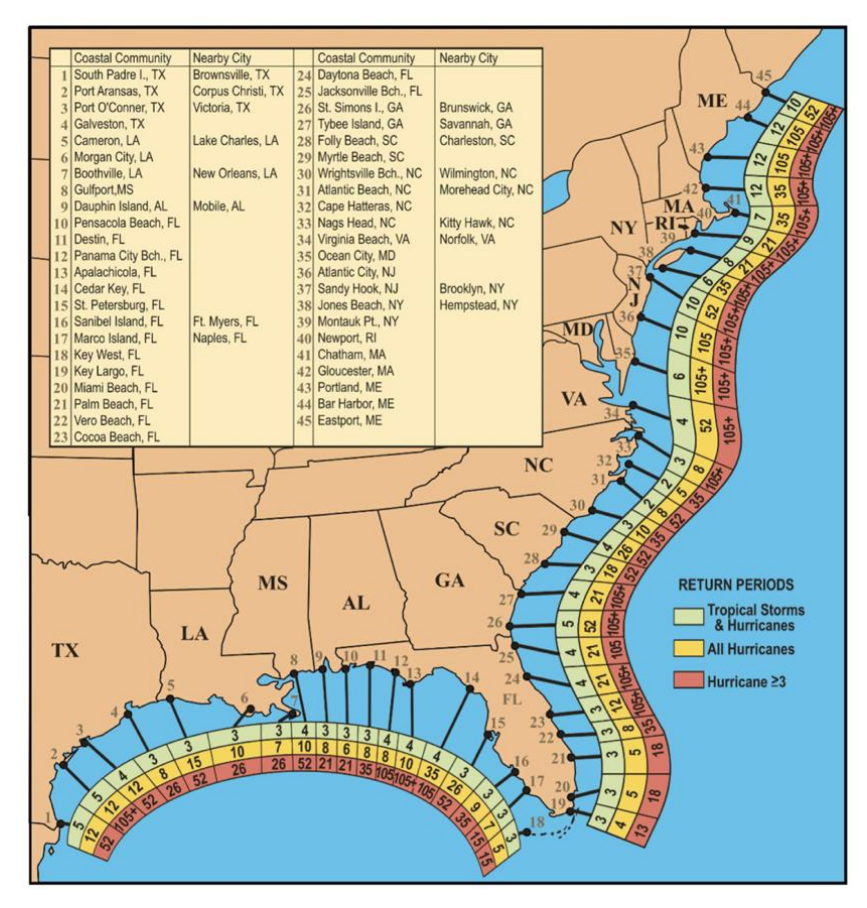


Figure 8: TC return periods (from Keim et al. 2007)

**Table 2:** Archeological sites in coastal Georgia under threat from different magnitudes of sealevel rise (from Howland and Thompson 2024)

	Tropical Storm	Category 1 Hurricane	Category 2 Hurricane	Category 3 Hurricane	Category 4 Hurricane	Category 5 Hurricane
Present Sea Level	953	1540	2661	3561	4058	4290
GMSL + 0.3 m	1201	1791	2852	3705	4193	4658
GMSL + 1.0 m	1615	2082	3057	3866	4309	4791
GMSL + 2.0 m	1898	2250	3191	3967	4397	4892

https://doi.org/10.1371/journal.pone.0297178.t001

ISO_TIME	NATURE	LAT	LON	WMO WIND			USA PRES		
18:00:00	TS	29.10	-78.00	110		110		115	
21:00:00	TS	29.30	-78.30			113		115	
1898-10-02 00:00:00	TS	29.60	-78.70	115		115		115	
03:00:00	TS	29.70	-79.10			115		115	
06:00:00	TS	29.90	-79.60	115		115		115	
09:00:00	TS	30.10	-80.10			115		115	
12:00:00	TS	30.40	-80.60	115	938	115	938	115	938
15:00:00	TS	30.80	-81.20			115	938	103	
16:00:00	TS	30.90	-81.40	115	938	115	938	98	
18:00:00	TS	31.10	-81.80	90		90		90	
21:00:00	TS	31.50	-82.50			78		78	
1898-10-03 00:00:00	TS	31.90	-83.10	65		65		65	
03:00:00	TS	32.30	-83.70			55		55	

Figure 9: Raw data for the 1898 TC from HURDAT2

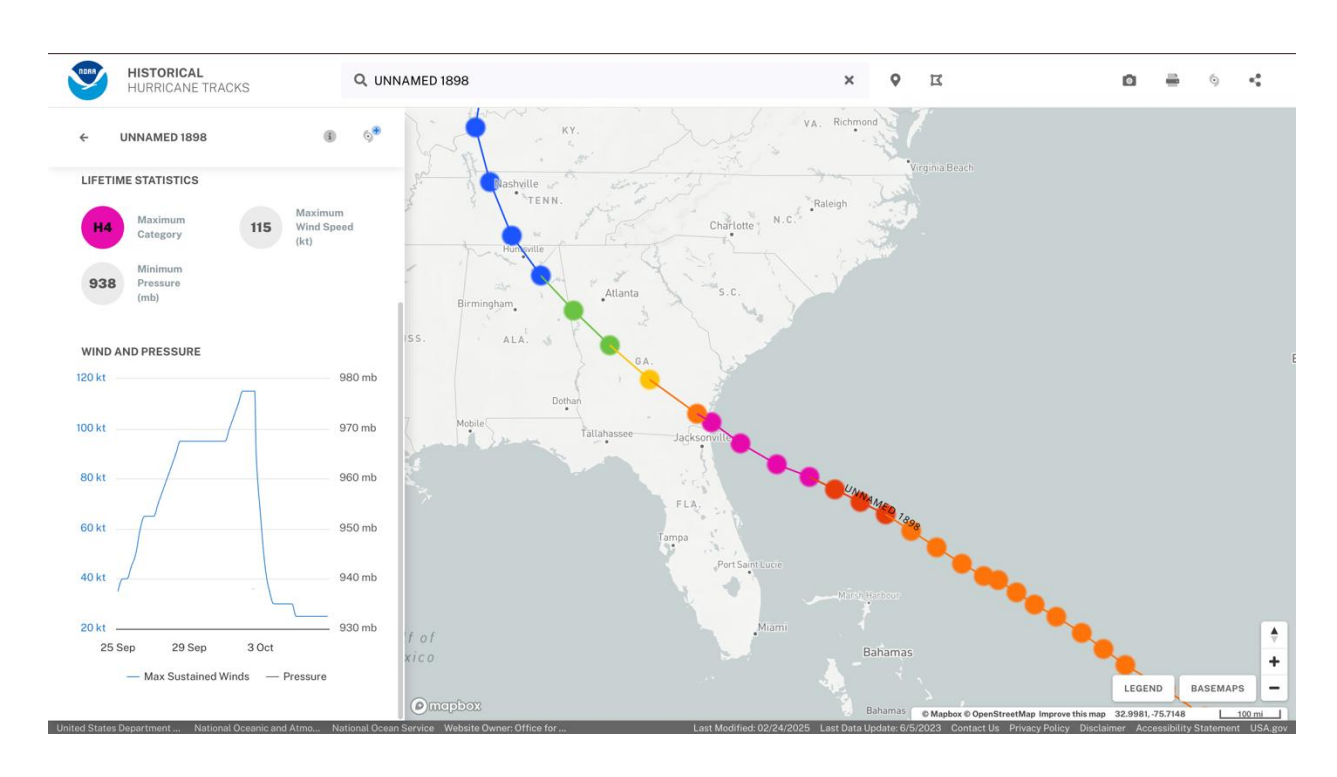


Figure 10: IBRTaCS visualization of the 1898 TC

#### **CHAPTER 3**

#### **METHODOLOGY**

#### **Case Selection and Data Sources**

The Georgia Hurricane of 1898 was recorded as a category 4 major TC that formed near the Lesser Antilles around 25 September 1898 and dissipated on 6 October 1898 near Newfoundland, Canada (IBTRaCS, HURDAT2). Atmospheric reanalysis data for the storm is available through the NOAA/CIRES/DOE 20<sup>th</sup> Century Reanalysis version 3 dataset (20CRv3). 20CRv3 has large improvements over predecessors and offers a spatial resolution around 1 x 1 degrees with 3-hour temporal resolution between 1851 and 2015 (Slivinski et al. 2019). Despite its name, it is one of the few datasets with data based on observations back to the mid-19<sup>th</sup> century. The 20CRv3 dataset has 28 pressure levels between 1000 and 1 hPa with four soil levels extending from 0 to 100 cm below ground. The dataset uses prescribed SSTs from HadISST2 before 1981 with daily SSTs interpolated from monthly values. As the dates of interest for this study are in late September and early October in the mid-latitudes, sea ice is assumed to be negligible. The numerical model used in the 20CRv3 is the Global Forecast System (GFS) version 14.0.1 (NOAA; Slivinski et al. 2019). The 20CRv3 reanalysis has a Cylindrical Equidistant projection with global coverage.

The 20CRv3 dataset was chosen for reanalysis as it is the only dataset at the time of this study that had sufficient atmospheric data to initialize the model runs in the study. The dataset also includes 80 ensemble members which helps account for uncertainty in conditions with few in-situ observations. Furthermore, the global coverage of the dataset was useful as the model domains could be adjusted throughout the study without needing other datasets.

#### The WRF-ARW Model

The Weather Research and Forecasting (WRF) model (Skamarock and Klemp 2007) is a state-of-the-art numerical mesoscale weather model with two available dynamical cores, data assimilation, and other utilities designed for applications ranging from atmospheric chemistry to fire weather. WRF is both a research and operational model, with its Advanced-Research WRF (ARW) dynamical core serving operational mesoscale and rapid refresh models such as the Rapid Refresh Model and the High-Resolution Rapid Refresh (HRRR) model (Dowell et al. 2022; James et al. 2022; Benjamin et al. 2016).

The WRF-ARW model was used in this study to dynamically downscale 20CRv3 data from ~11 km grid size, down to a grid size around 2.2 km. Most reanalysis literature that primarily uses the WRF is focused on more recent storms. In 2010, WRF was run using 20th century reanalysis data to examine a historical New England TC landfall in 1938 (Hart 2010). A 2013 study used the WRF to simulate the Blizzard of 1888 with promising results (Michaelis and Lackmann 2013). Michaelis and Lackmann noted a lack of model accuracy in storm track. While there are limited observations from the 1898 TC, the use of WRF-ARW model for reanalysis is well-documented, and the above studies justify its use for this study.

## **Model Parameterizations and Physics**

The options chosen for the WRF-ARW simulations are critical for accurately modeling atmospheric processes associated with TCs. Minuscule changes in parameterization or physical schema can produce a radically altered storm. For this study, the WRF-ARW user manual's "best-practices" for TCs were followed to ensure realistic results (WRF-ARW Users Guide, NCAR MMM 2023).

The physics options of the WRF-ARW allow for parameterizing smaller-than-grid phenomena (microphysics) and less-important phenomena so that computational efficiency can be increased. For this study, physical parameterizations were kept consistent regardless of model run. The changes occur when moving between domains. For instance, with the parent domain (d01), the grid-cells are larger than many mesoscale processes such as cumulus convection, so these processes must be parameterized. However, on runs with a resolution of less than 3 km, cumulus convection is resolved because grid-cells are small enough to be convection permitting. Hence, in the smaller domains, physics options relating to convection are set to '0' to tell the model that parametrization is not needed. However, even smaller domains require some parameterization, especially regarding microphysics.

There are 5 major physical components that default to parameterization in WRF. For this study, the 'tropical' physics suite was used in WRF-ARW. This pre-programmed suite includes the parameters deemed by WRF developers to best represent tropical systems (Table 3). The use of a predefined suite also limited variation in the model caused by using a custom suite that might not have the best options for the given case study. One important sensitivity for tropical cyclones in WRF-ARW is the microphysics and planetary boundary layer (PBL) parameterization schemes

**Table 3:** WRF-ARW parameterization settings used for this study

WRF Physics Settings	Domain 1	Domain 2			
<b>Cumulus Convection</b>	Tiedtke	No Parameterization			
Microphysics	WSM6 (Hong and Lim 2006)	WSM6 (Hong and Lim 2006)			
Radiation	RRTMG LW/SW	RRTMG LW/SW			
PBL	YSU PBL (Hong 2007)	YSU PBL (Hong 2007)			
Surface Layer	MM5 (Zhang and Anthes 1982)	MM5 (Zhang and Anthes 1982)			
LSM	Noah LSM (Chen and Dudhia 2000)	Noah LSM (Chen and Dudhia 2000)			

used, especially in real-data cases such as this study (WRF-ARW Users Guide, NCAR MMM, 2023). For consistency in this study, WRF options were not altered besides turning off the convective parameterization on the smaller domain 2.

#### **Model Domains**

Because of the dynamic and relatively small-scale nature of TCs, the WRF-ARW was run with a 2-domain configuration with a parent domain (D01, 11 km resolution) and a vortex-following child-domain (D02, ~2.2 km resolution). The vortex-following software tracks a TC based on the lowest pressure within the starting area of the VF domain. Since the vortex-following domain is primarily used for TCs, the model outputs (along with normal variables) a list including the coordinates of the vortex center (latitude, longitude), minimum mean sea-level pressure (mb), and maximum 10-meter winds (m/s). The vortex-tracking algorithm used within WRF appears to be adopted from Shuyi Chen and colleagues' implementation of hurricane tracking in the MM5 model. Furthermore, the MM5 algorithm seemed to follow the methodology of Kurihara et al. (1998). There were notably decreased computational requirements for higher resolution simulations and a beneficial central location of the vortex across all time frames giving consistent viewing angles over time.

There were several "best-practices" taken from the WRF-ARW Users Guide to create the domain for the study. First, the larger parent domain was extended to a size large enough to capture large-scale synoptic patterns responsible for steering the TC. Also, boundary conditions can be affected by mountain ranges (such as the Rocky Mountains). As such, the model boundaries were positioned over the ocean where possible. In the case of the vortex-following child domain, no user input was supplied to the model to steer the domain. The child domain was initialized entirely over the ocean to capture the TC vortex early in the model run (Fig. 11).



**Figure 11:** D01 (larger) and the vortex-following D02 (smaller) used in this study.

## **Initializing WRF with 20CRv3**

Despite 20CRv3 data being output from the Global Forecasting System (GFS) medium-range weather model, initializing WRF with these data was not a straightforward process. The file format 20CRv3 is available in (netCDF4) does not match the input format WRF-WPS expects (GRIB2). To get around this incompatibility, the pyWinter package (created by dinolash, on Github) was used to re-format the netCDF4 data into GRIB2 files for processing by WRF-WPS.

To run WRF, several atmospheric and surface variables are required. These variables were all obtained from 20CRv3. The 2D input variables used in this study were surface pressure, mean sea-level pressure, 2-meter relative humidity, 2-meter temperature, surface temperature, 10-meter U and V winds, and water-equivalent snow depth (this was required to run WRF, but not important in this study). The 3D inputs were geopotential height (isobaric), volumetric soil moisture (depth below land layer), specific humidity (isobaric), temperature (isobaric), soil temperature (depth

below land layer), U-winds (isobaric), and V-winds (isobaric). All 3D variables had 28 isobaric pressure coordinates (except soil related variables with 2 levels (0 and 1m) and specific humidity with 22 levels). Once the variables were selected, they were filtered to the year 1898 to only include values relevant to this study (20CRv3 data on Derecho is packaged in yearly files).

#### **Spectral Nudging**

On the first few model-run trials, the modeled TC was not following what was expected with the 1898 TC in either track or intensity. Thus, spectral nudging was employed under recommendation and guidance from the WRF-ARW User's Guide to try to nudge the model towards the 20CRv3 observations. Spectral nudging has been shown to improve both large and small scale WRF-ARW simulation performance when using the proper wavenumber (Liu et al. 2012). For this study, all wavenumbers were set to the best-practice settings from the WRF-ARW Users Guide. Spectral nudging was set to occur during the first 24 hours of the model run before it was gradually tapered off.

While preliminary WRF model runs with no nudging produced storms with inconsistent tracks making landfall as far north as North Carolina, employing spectral nudging to the model greatly enhanced the track accuracy of the modeled storm relative to the 20CRv3 input data. Unfortunately, lack of observations on storm intensity leaves little comparison for how the spectral nudging helped with storm intensity. Spectral nudging was used for all subsequent model runs, including those forced by present-day and future climate conditions.

Spectral nudging has been employed in several studies to help improve model accuracy. For instance, a 2024 study near the Great Lakes used spectral nudging to correct a cold bias in a WRF-based regional climate model with promising results (Hutson et al. 2024). For TCs, spectral

nudging was used in a rapid intensification study on Typhoon Megi (2010) where it was employed to nudge large-scale flow closer to reanalyzed values (Wang and Wang 2014).

## **Stochastic Kinetic-Energy Backscatter Scheme (SKEBS)**

While the 20CRv3 dataset was comprised of 80 ensemble members, the individual files were quite large and beyond the computing limits for this study. Given the already uncertain nature of atmospheric data from 1898, uncertainty in the WRF model itself was most important to this study. The Stochastic Kinetic-Energy Backscatter Scheme (SKEBS; Shutts 2005; Berner et al. 2009) was used to generate perturbations in initial conditions for the WRF-ARW model. The scheme was used to generate 16 unique ensemble members for the modeled 1898 storm. Four members were also created for runs perturbed by climate data (see next section). Only 4 members were used in climate scenarios because of constraints on computational time on the Derecho supercomputer. SKEBS works during model integration by randomly perturbing various physical parameterizations to help quantify model uncertainty. In this study, the WRF-ARW default settings for SKEBS were used and only the seeds for the random perturbations were changed.

SKEBS is useful for this study as its WRF-ARW implementation perturbs rotational wind, potential temperature, temperature, orographic waves, convection, and more (Skamarock et al. 2019). Furthermore, SKEBS is particularly useful in areas of the free atmosphere and is not as limited as other options in WRF (such as SPPT, stochastically perturbed physics tendencies) to areas of "high tendencies," such as those found around thunderstorms and TCs (Berner et al. 2015). SKEBS has been used to produce ensemble spread in WRF before. SKEBS produced large variation in TC track and intensity in a 2019 study on Hurricane Earl (Li et al. 2019).

## Pseudo Global Warming (PGW)

To simulate the effects of a future climate on the 1898 Georgia TC, we employed the pseudo global warming method (Brogli et al. 2023). Using data from the Community Earth Systems Model Large Ensemble (CESM2-LENS), differences between 1888-1898 and 2084-2094 decadal averages were calculated and then added to the WRF model's initialization data to simulate climate change. All 16 variables used to initialize WRF were perturbed using PGW.

For all 2D and 3D input data (including atmospheric and land variables), the description of the 20CRv3 target grid was extracted from the 20CRv3 data using Climate Data Operator's (cdo) griddes function and saved to a file for the regridder. Two-dimensional variables at a given level are regridded based on latitude and longitude from the latlon grid of CESM2 to the Gaussian grid of 20CRv3 using cdo. Two-dimensional regridding is relatively straightforward as it is a native task for most earth system gridding software, including cdo. For 3-dimensional data, the process was a bit more involved as 3D "reboxing" is not native to cdo. First, the ensemble members were averaged along their time axis to produce the decadal average for each era, respectively. Then, differences between eras were calculated to produce the pseudo-global-warming (PGW) effect. There were 2 steps for the regridding of the 3D data. First was horizontal regridding which used included grid weights in the CESM2 data and the cdo remapbil function. Secondly, the data were regridded vertically from ~41 levels in CESM2 to 28 isobaric levels native to 20CRv3. This was done by using cdo's built-in intlev function and manually entering the isobaric coordinates of 20CRv3 output.

Implementing PGW into 20CRv3 involved simple Python script using xarray and numpy. First, because of memory restrictions, the 20CRv3 data were sliced to only include the times around the 1898 TC. Once sliced, the 20CRv3 data and regridded CESM2 perturbations were

loaded into memory. To simulate PGW, the perturbations were added to 20CRv3 by separating the variable from the dataset and setting NaNs to 0 before summing 20CRv3 and the perturbations. Afterwards, the data were reattached to the native 20CRv3 grid to be processed by WRF-WPS. PGW was used to perturb every variable available from 20CRv3. There were three timeframes chosen for this study, two of which were perturbed by CESM2-LENS climate data:

- The 1898 timeframe encompasses the storm as it occurred in 1898 with the climate conditions of 1898. The data for the model 1898 was entirely from the 20CRv3 dataset and unaffected by climate data.
- The 2024 timeframe (hereafter "present-day") is a WRF simulation of the 1898 Georgia TC if it were implanted in today's climate as as projected by CESM2-LENS following the SSP370 socioeconomic pathway (O'Neill et al. 2017). The present-day run was forced via PGW using CESM2-LENS data by subtracting historical CESM2-LENS climate conditions (average from 1890 to 1899) from present-day CESM2-LENS climate conditions (average from 2015 to 2024).
- The 2098 timeframe (hereafter "future") is a WRF simulation of the 1898 Georgia TC if it were implanted in the climate of 2098. Like the present-day simulation, this run was also forced via PGW by subtracting historical CESM2-LENS climate conditions (1890-1899) from future CESM2-LENS climate conditions (average from 2085-2094).

In both PGW cases, a "delta" file was created for each variable before it was re-gridded and added to unperturbed 20CRv3 data via steps mentioned in previous paragraphs. The variables altered by PGW include all 16 input variables as required by WRF (see section *Initializing WRF with 20CRv3* for a list of variables). It should be noted that, while 10m U-winds from CESM2-LENS were available on Derecho, 10m V-winds were not. Furthermore, the v-winds were not

available from any of the CESM2-LENS data repositories. To fill in for the missing 10m wind data, 10m winds were assumed from the lowest pressure level of the isobaric U and V winds (1000 mb). While in most cases these perturbations were very small, they were still added to the model data for thoroughness.

### The Sea Lake and Overland Surges from Hurricanes (SLOSH) Model

To model storm surge from WRF-ARW storms, this study used the Sea Lake and Overland Surges from Hurricanes (SLOSH) model provided by NOAA (Jelesnianski et al. 1992). SLOSH has its own parametric wind model, so its calculations do not directly depend on WRF-ARW wind data, but rather high-level products derived from WRF runs. For this study, SLOSH also allows for direct comparison of the output from this study to NOAA's official storm surge maps which were also made using SLOSH (refer to Fig. 7).

Four variables are required to run SLOSH: latitude, longitude, change in pressure from environment, and radius of maximum winds. These 4 variables were extracted from the WRF model ensemble means (made by averaging all ATCF output files for every ensemble member) and used to initialize SLOSH. Pressure change from the environment was calculated by subtracting MSLP from 1013.25 mb (a standard atmosphere). The values themselves were produced by the vortex-following software to maintain uniformity in the definition of a best-guess storm. For this study, SLOSH defaulted to the 1929 National Geodetic Vertical Datum for storm surge depth. This measurement is height above mean sea level but uses the mean sea level of 1929. This is important when considering the future effects of storm surge as sea level has risen (and is continuing to rise) since 1929.

### **CHAPTER 4**

#### RESULTS

## Modeling of the Storm: October 1-4, 1898

The first modeled timestep for all model runs of the storm (including the climate forced runs) is at 1200 UTC 01 Oct (Fig. 12A). At this time, the center of circulation was a few hundred kilometers northeast of Nassau in the Bahamas. In 800 mb GPH contours, the initial WRF-ARW TC was positioned just northwest of the cyclone in the 20CRv3 dataset (Fig. 12B). The 800 mb pressure surface was chosen to avoid contamination in surface variables by the Appalachian Mountains which were in the parent domain at the first timestep. The 1-hour difference in the two images should be noted here as it is likely this difference is partially responsible for the difference in the storm center location. The modeled 1898 TC followed closely to the HURDAT2 recorded track closely but was further north towards the track in the 20CRv3 dataset (Fig. 13). Nudging in the track of the cyclone in WRF-ARW is evident in the first few datapoints as the track more closely follows the erratic 20CRv3 storm. This nudging tapers off over the course of the model run resulting in a smoother track around landfall (Fig. 14).

All 16 ensemble members had the storm making landfall in or around Brunswick, Georgia. Most of the deviation in the track was latitudinal and limited to between 10 and 20 km in either direction (Fig. 14). Of note early in the storm's track was a slight turn to the west over the ocean followed immediately by a slight northerly turn. Despite this initial wobble in the storm's track, it is evident that the modeled storm made a nearly perpendicular landfall later in the simulation. This perpendicular landfall indicates that the modeled storm's maximum impacts (including its forward speed) were felt along the coast. The estimated forward speed of the modeled storm varied from around 20 knots over open water to 6 knots inland. This forward speed is an important component

of rainfall totals in later sections. At landfall (10 UTC Oct. 2), the modeled storm's forward speed was around 16 knots (Fig. 15).

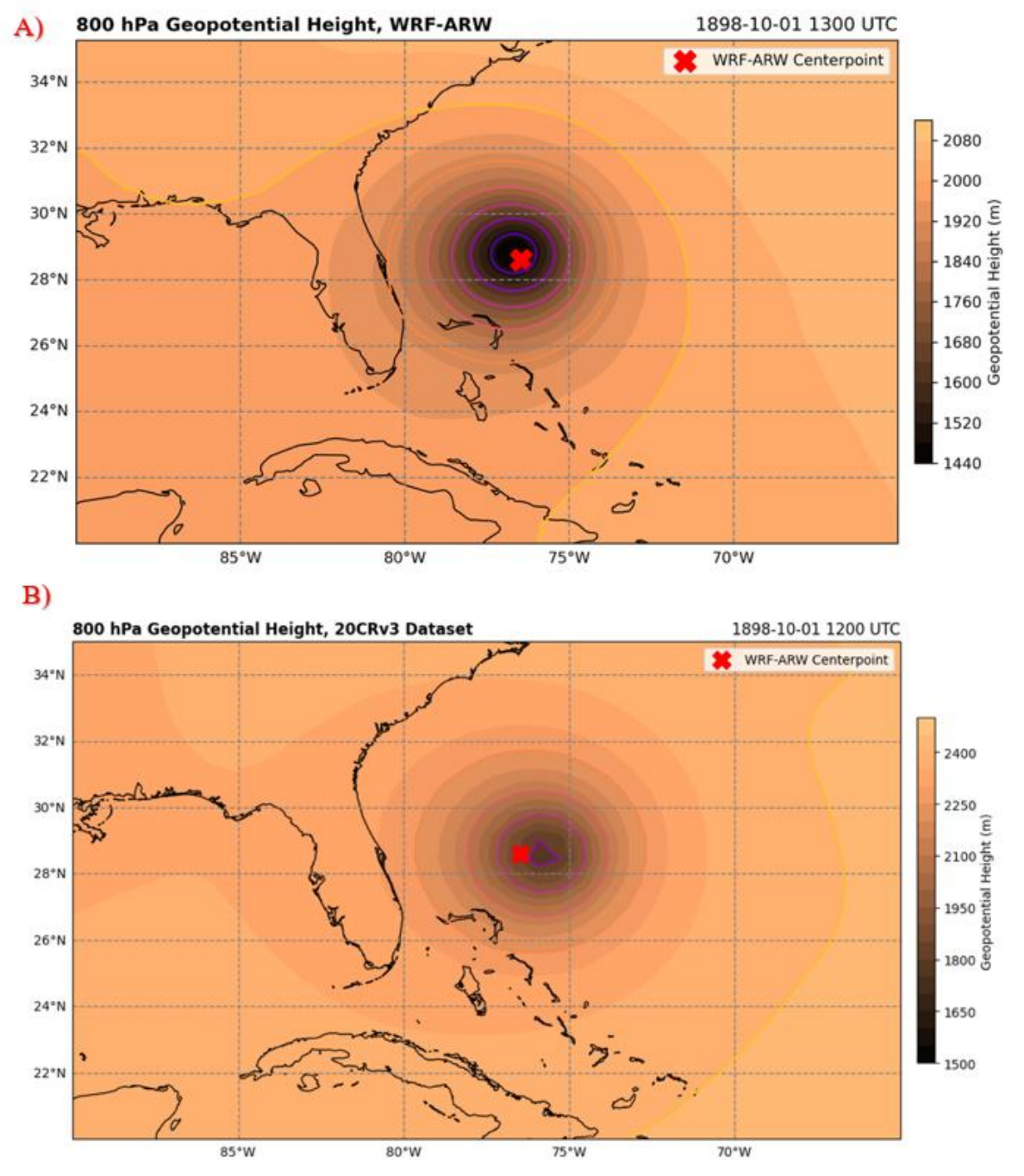


**Figure 12:** 800 mb geopotential height contours from WRF-ARW (A) and 20CRv3 (B). The red 'X' represents the storm center from WRF-ARW

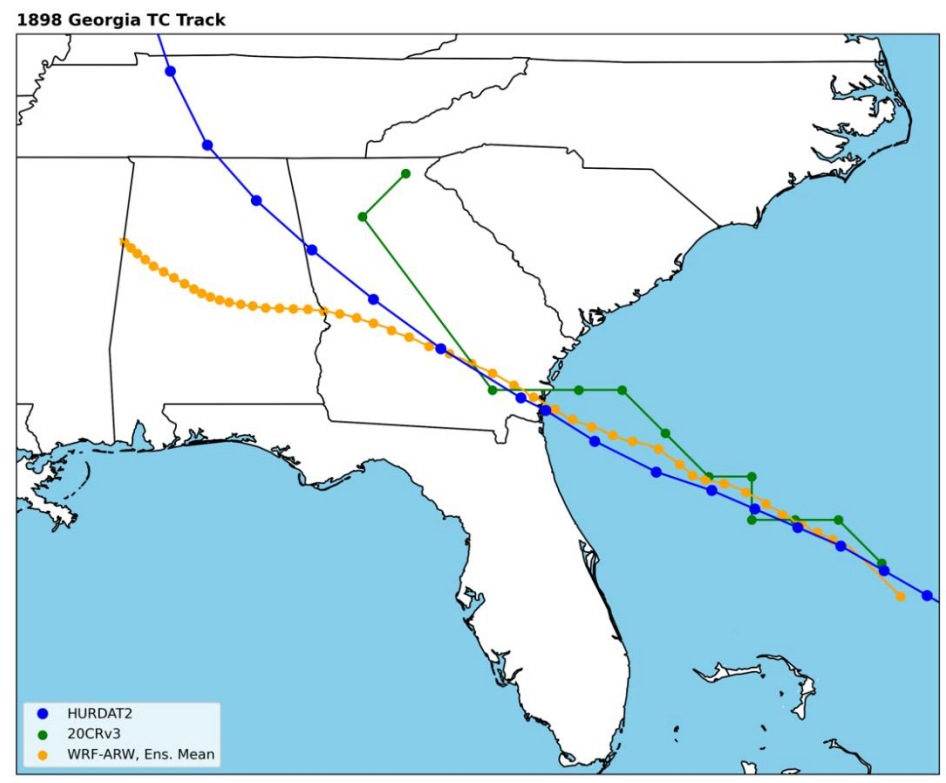


Figure 13: 1898 TC tracks from HURDAT2, 20CRv3, and WRF-ARW

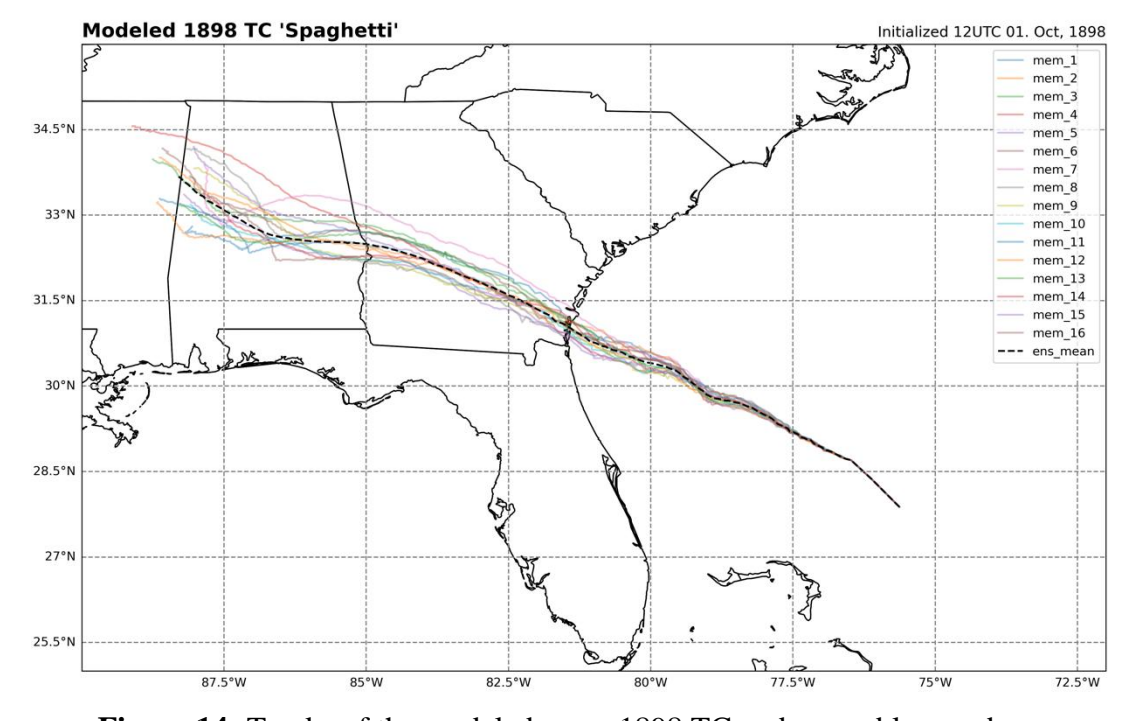


Figure 14: Tracks of the modeled mean 1898 TC and ensemble members

The storm's minimum central pressure was lowest (~948 mb) across the ensemble at model initialization. Over time, the pressure increased to around 952 mb where it decreased slightly to a secondary minimum of 950 mb around 0600 UTC on 02 Oct. Afterwards, the storm's minimum pressure began its final increasing trend suggesting interaction with terrain. Sandrik and Landsea (2003) inferred a landfalling MSLP of 938 mb. However, both reanalysis and modeling in this study showed a landfalling storm with an MSLP of around 955 mb (Fig. 16).

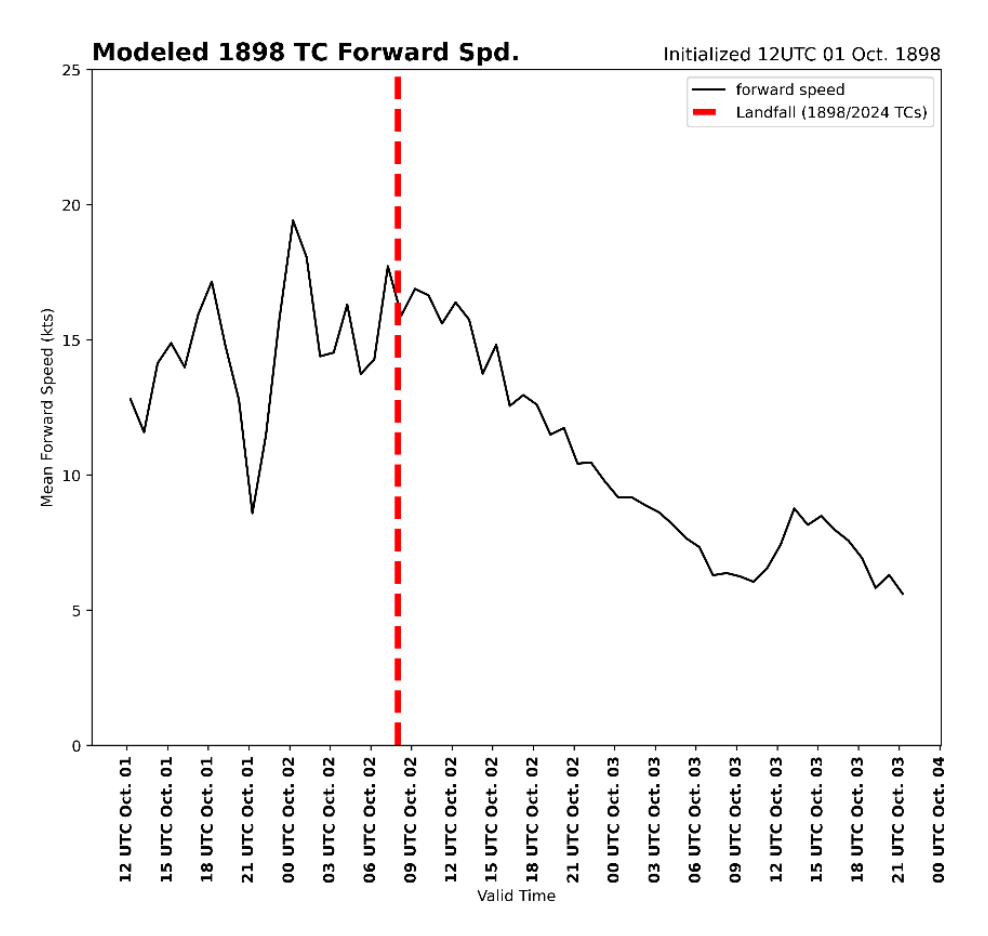


Figure 15: The 1898 TC's mean forward speed

The intensity of the modeled 1898 TC was lower across all metrics compared to the information in HURDAT2. At landfall, the storm's MSLP was ~954 mb. While the storm was labeled a category 4 by Sandrik and Landsea (2003), the WRF-ARW ensemble struggled to

produce a weak category 3 storm (by wind speed) in even the most intense runs (Fig. 17). The modeled 1898 TC made landfall with mean winds around 70 knots, making it a category 1 hurricane.

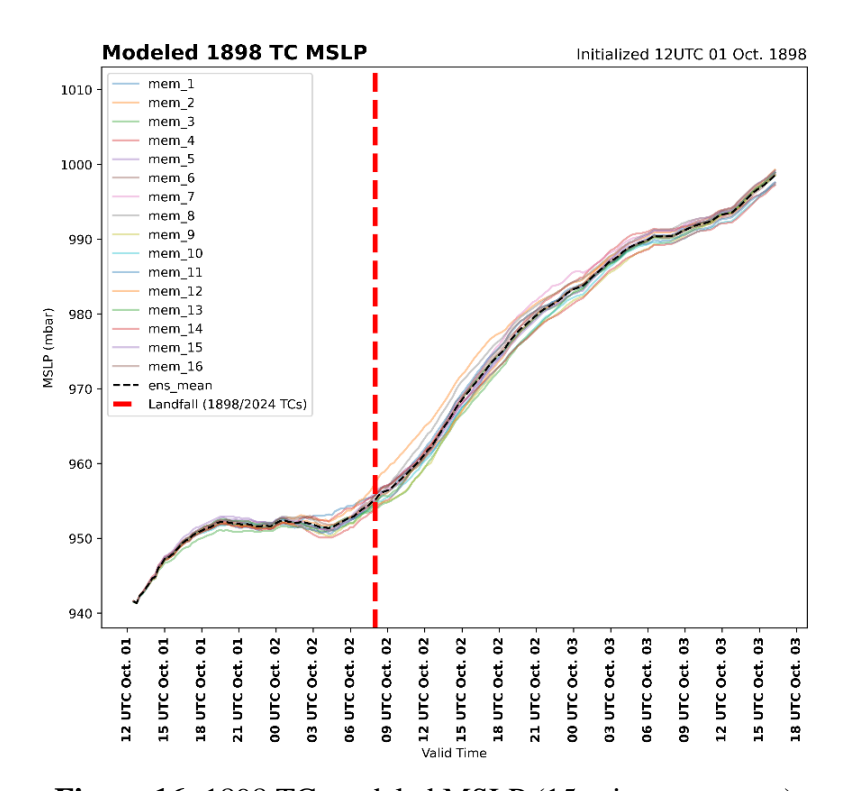
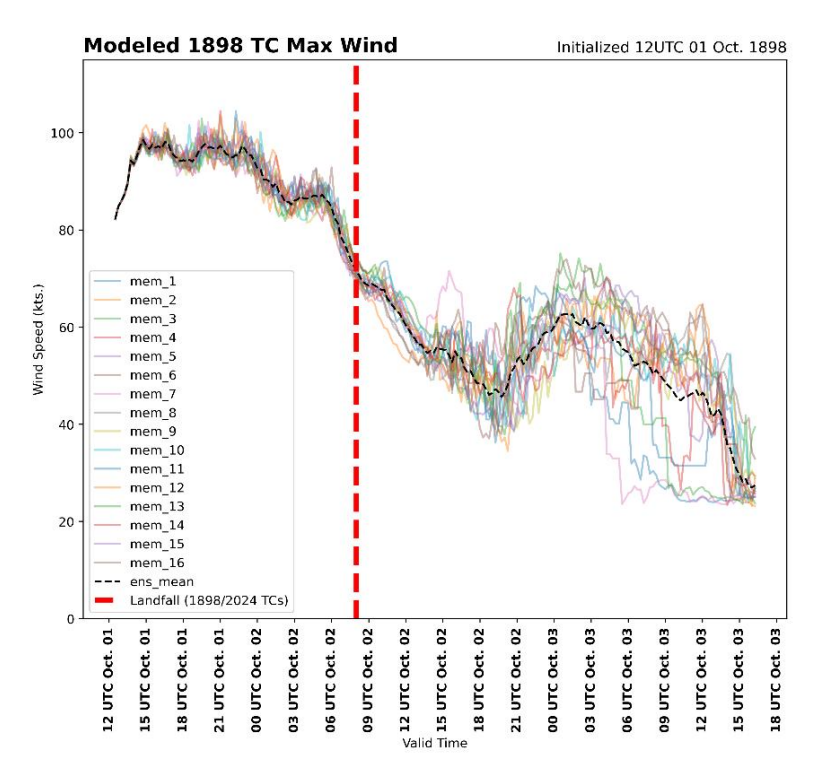


Figure 16: 1898 TC modeled MSLP (15-minute average)

The corridor of maximum winds for the modeled 1898 storm at landfall were mostly to the north of the eye. The wind field was quite large with the storm's highest winds extending north into central South Carolina (Fig. 18). The modeled TC produced relatively light rainfall along the Georgia coast. Most precipitation fell to the north of the modeled 1898 storm along its path with a maximum onshore amount of around 5 inches in a narrow corridor between Brunswick and Savannah, GA. Greater rainfall accumulations occurred offshore with accumulations of 6-8 inches. Further south of Brunswick near Jacksonville, FL, the modeled rainfall amounts were between 2 and 3 inches (Fig. 19).



**Figure 17:** 1898 TC modeled maximum wind speed (15-minute average)

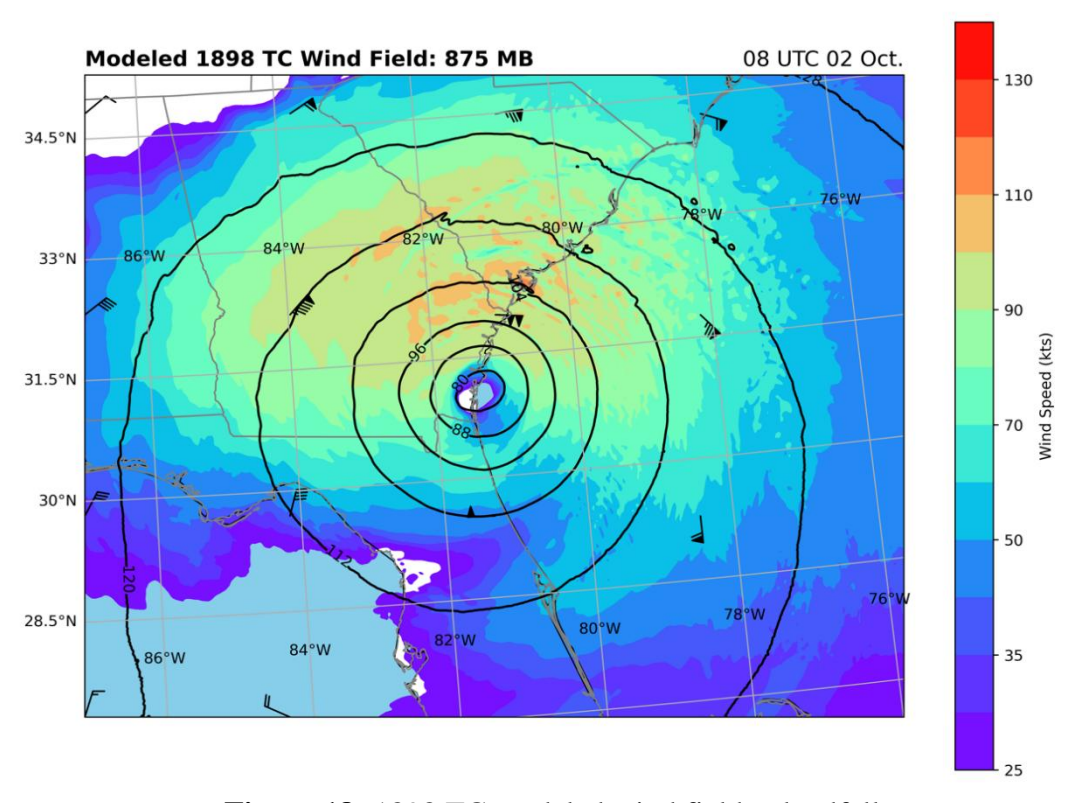
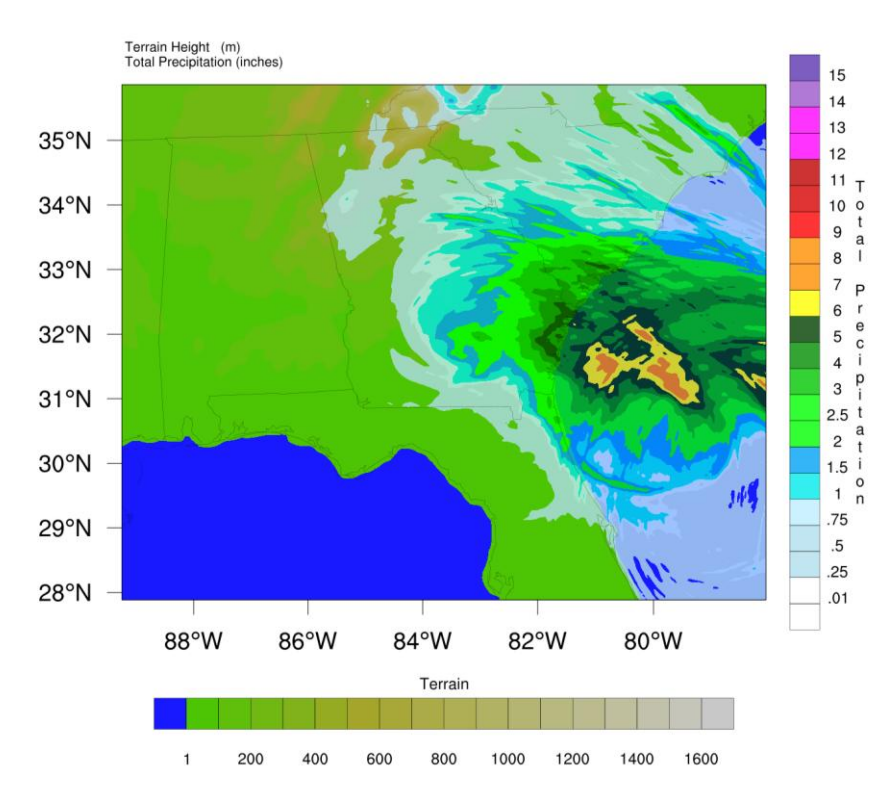


Figure 18: 1898 TC modeled wind field at landfall



**Figure 19:** 1898 TC run-total (~ 60 hours) modeled accumulated precipitation

Brunswick, GA had the lowest ensemble mean modeled surface pressure at ~960 mb (Fig. 20 A). The second lowest modeled MSLP was at Jacksonville, FL, around 970 mb (Fig. 20 B). Appreciable drops in pressure were also modeled in Savannah, GA (Fig. 20 C) and Charleston, SC (Fig. 20 D), where the lowest ensemble mean modeled MSLPs were ~980 mb and ~995 mb, respectively. Compared to the one MSLP observation of 29.02 inHg (982 mb) in Jacksonville, FL (Oct. 1898, U.S. Weather Bureau), there is the possibility that the modeled storm's pressure in Jacksonville was lower than observations (Fig. 20 B).

Windspeed in the modeled 1898 TC was taken from the model just offshore of selected cities along the coast from Jacksonville, FL to Charleston, SC (Fig. 21). The reasons behind choosing the offshore points for 10m winds were apparently unphysical differences in the pressures experienced in each city (at each city's respective latitude and longitude), and the 10m

windspeeds taken at those cities (see Discussion for more details). One feature in Brunswick, Jacksonville, and Savannah is the passage of the TC's eyewall marked by a sudden drop and rebound in windspeed with timing dependent on the city's location relative to the storm center. Overall, the strongest 10-meter winds in the model attained minimal hurricane force around Brunswick and Jacksonville with a mean speed of ~70 knots (Fig. 22 A, B). Modeled winds in Savannah were also hurricane-force and were around 65 knots at their strongest (Fig. 22 C). Further north in Charleston, modeled winds never exceeded 60 knots on average, suggesting the city likely did not experience hurricane-force winds (Fig. 22 D).

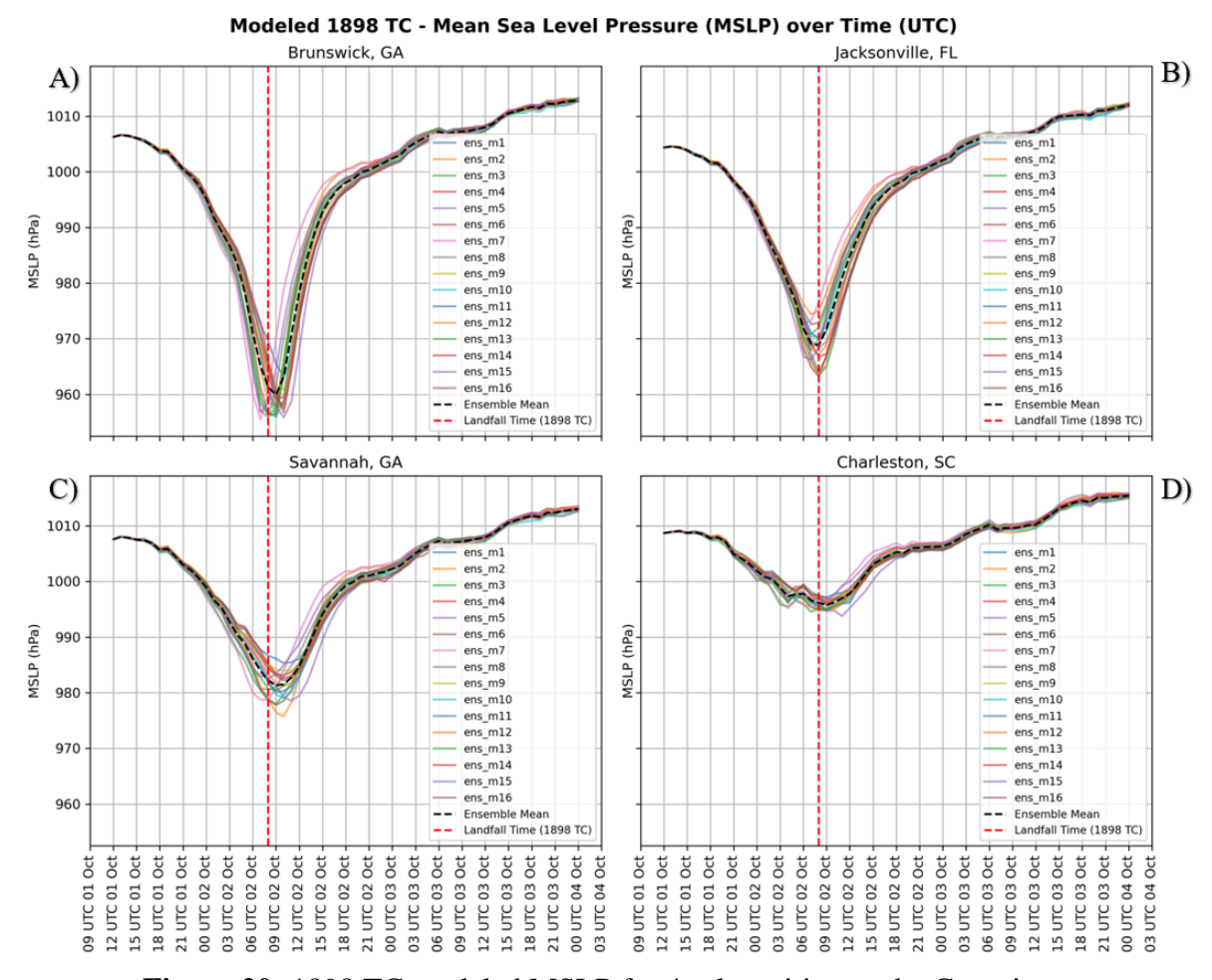
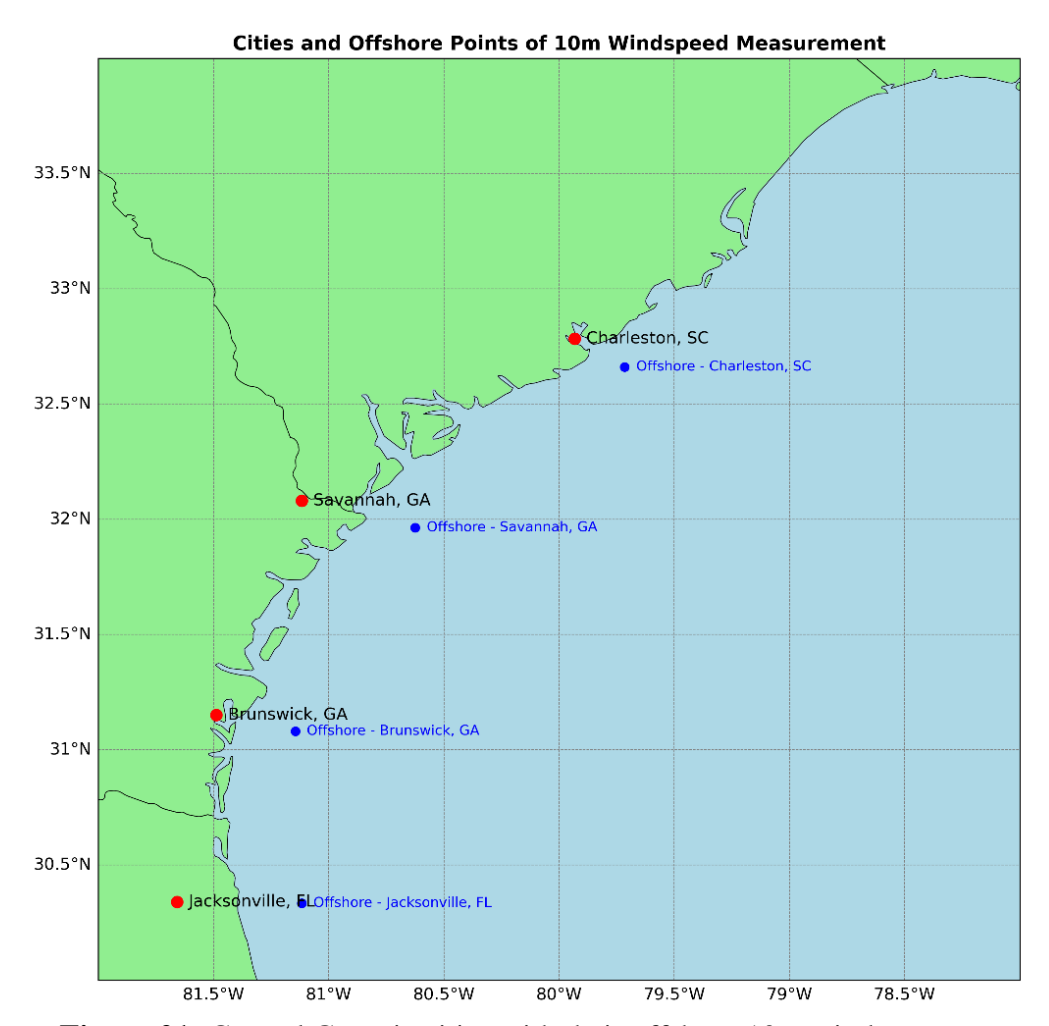


Figure 20: 1898 TC modeled MSLP for 4 select cities on the Georgia coast



**Figure 21:** Coastal Georgia cities with their offshore 10m wind measurement points

One of the records reportedly held by the 1898 Georgia TC was its storm surge at Brunswick, GA, which was estimated to be around 16-18 feet (Sandrik and Landsea 2003). Coupling a best-guess storm from the WRF ensemble mean produced in this study to SLOSH revealed a storm surge of similar depth and location. About an hour before modeled landfall in SLOSH, the effect of the barrier islands is apparent on surge with around 2 feet of difference in modeled surge. On the windward side of the islands, especially those in Glynn County, modeled surge is between 8 and 10 feet NGVD (National Geodetic Vertical Datum, 1929; height above mean sea level). On the islands' leeward side, modeled surge was between 6 and 8 feet (Fig. 23).

Modeled surge along the Georgia coast extended further north as well. In the Savannah/Tybee Island, GA area modeled surge was between 4 and 8 feet (Fig. 24). There was appreciable surge as far north as Jasper County, SC (Figs. 23, 24).

At landfall, the modeled storm surge in and north of the Brunswick, GA area was between 12 and 14 feet. There is also upstream propagation of the surge into tidal estuaries. The inland extent of the surge was exacerbated to the north of Brunswick, where the corridor of maximum onshore flow was located (Fig. 23, Fig. 24). The coastal area experiencing the greatest impact from

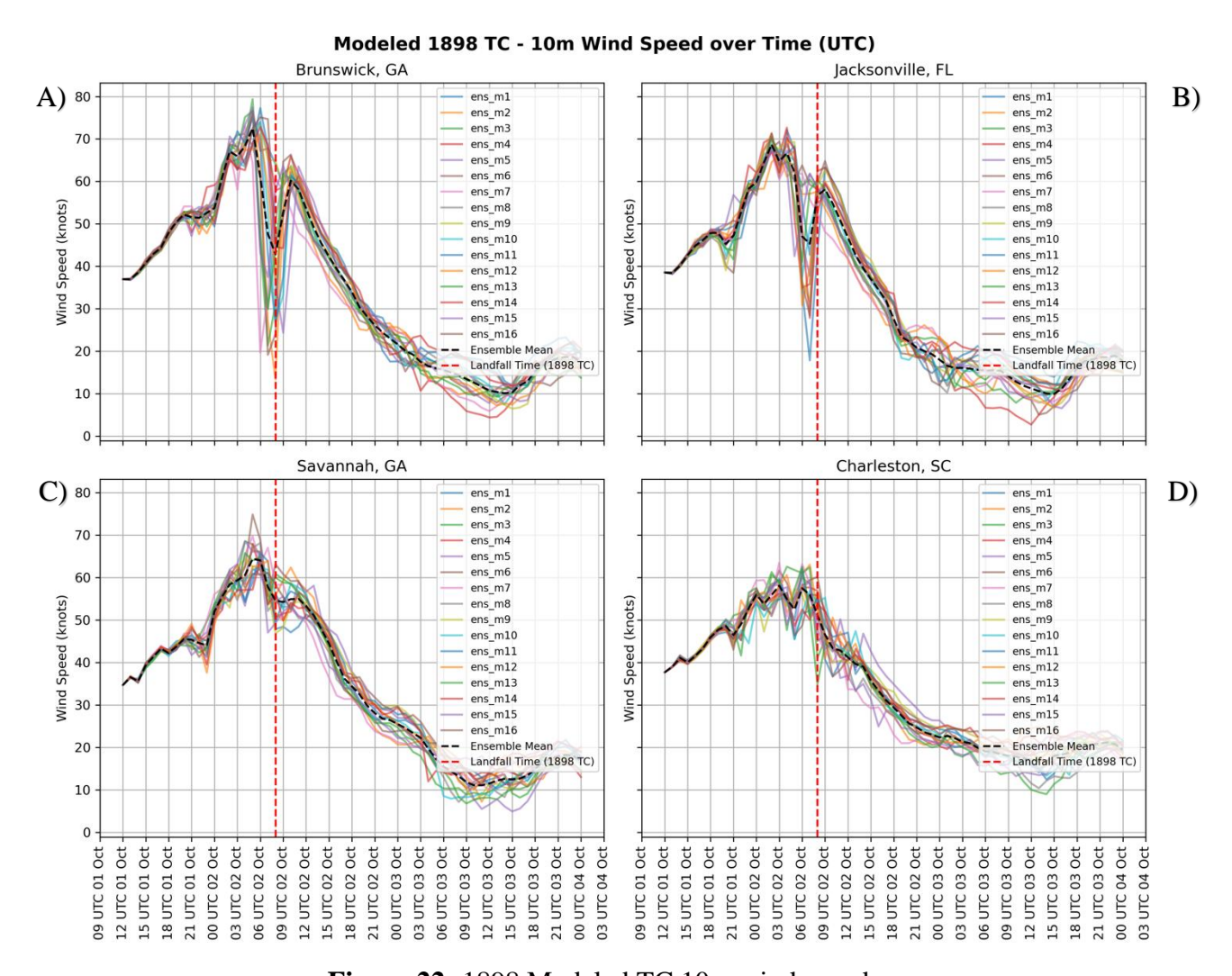


Figure 22: 1898 Modeled TC 10m wind speeds

modeled surge was the mouth of the Altamaha River, just south of Darien, GA. Islands in the area that were impacted were St. Simon's Island and Little Saint Simon's Island, both of which received 10-14 feet of modeled storm surge (Fig. 24).

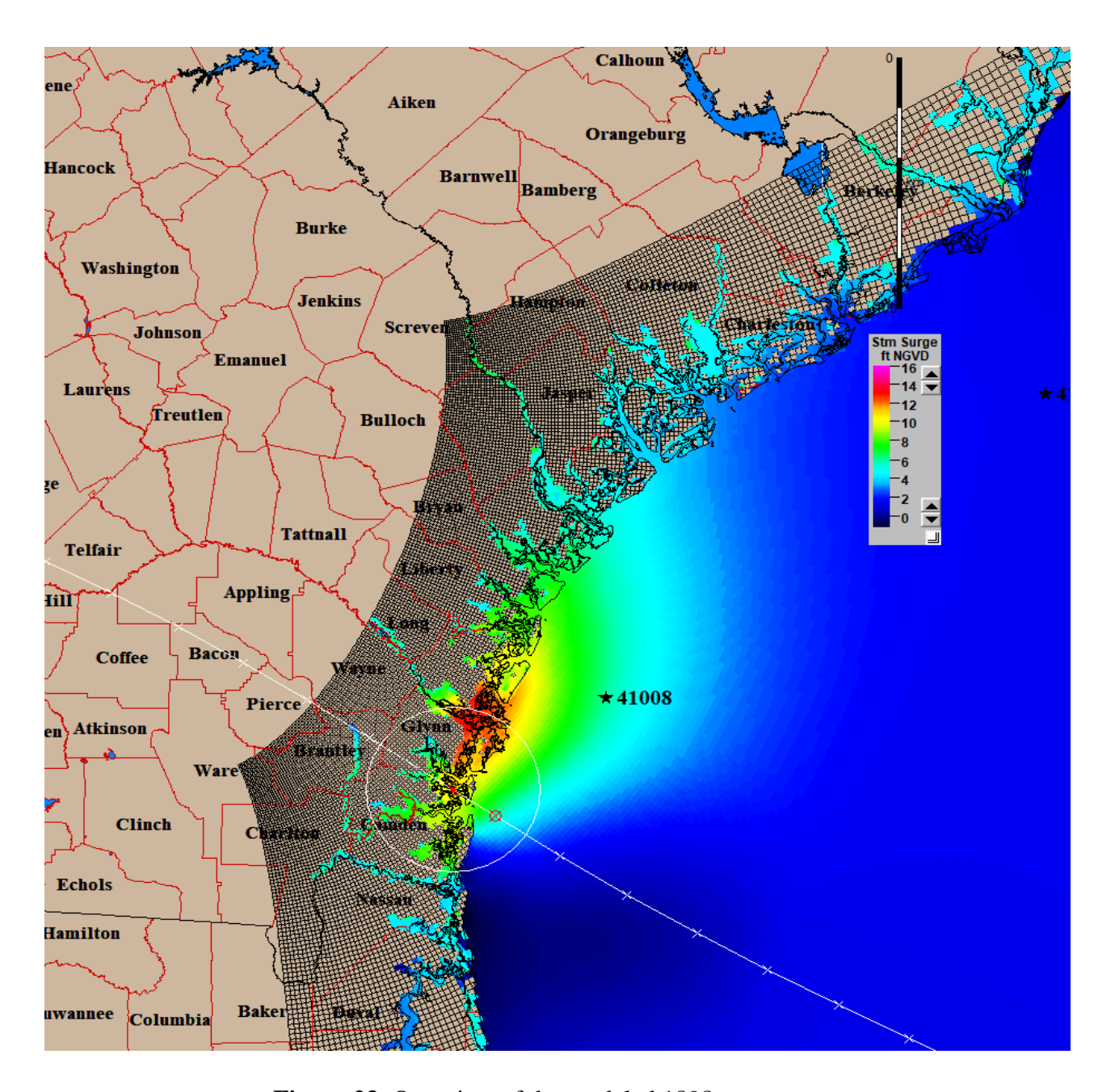


Figure 23: Overview of the modeled 1898 storm surge

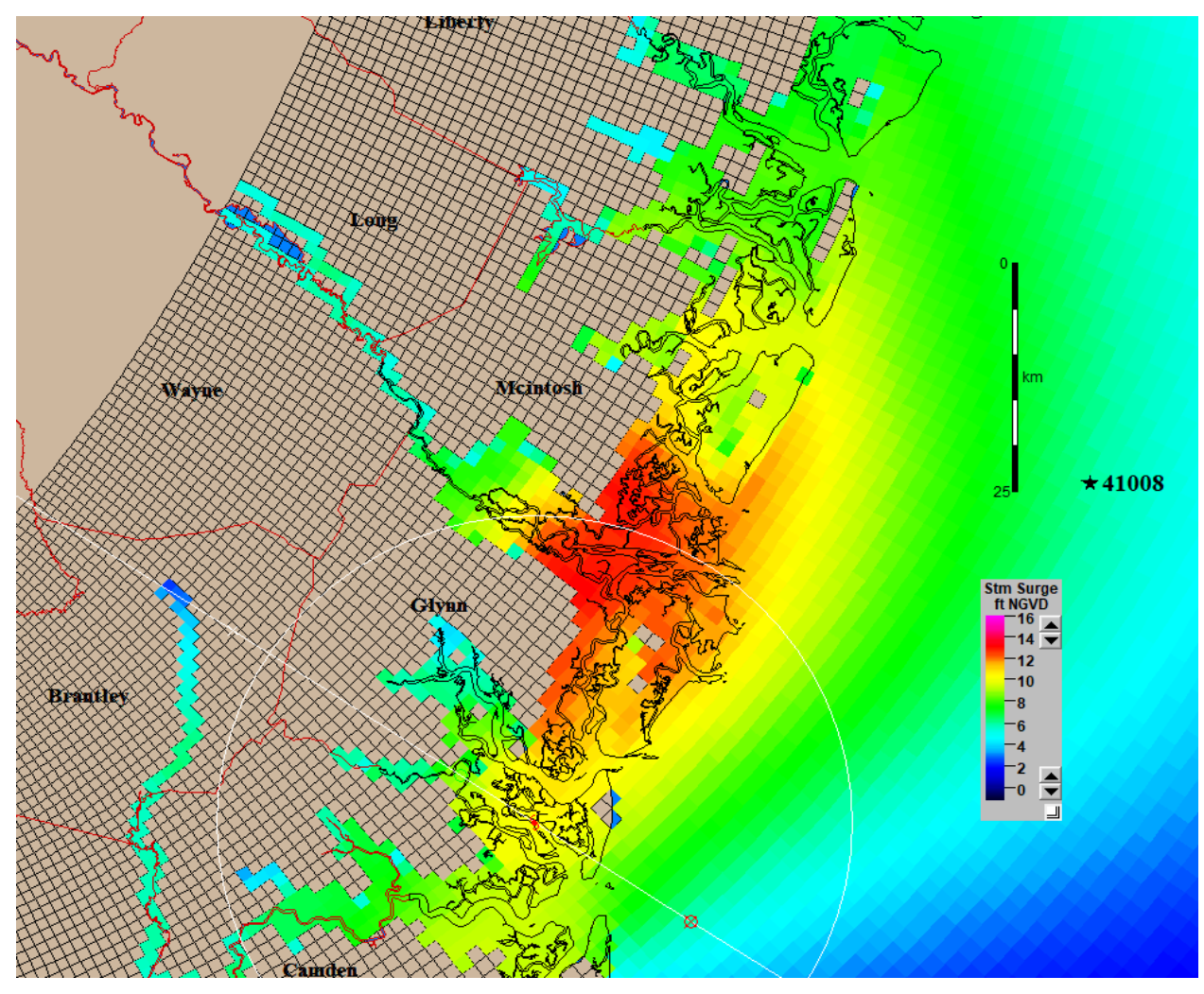


Figure 24: Same as Figure 23 but zoomed on the Brunswick, GA area

# SSP 370: 1898 TC in Present-day Climate Conditions (2024)

When the modeled 1898 TC was forced with present-day (2024) climate conditions, the storm made landfall almost identically with the modeled 1898 TC at around 9 UTC Oct. 2. Brunswick, GA remained near the center of the ensemble mean landfall, although there were a few more southerly ensemble members during this simulation (Fig. 25). The modeled 2024 TC also had near identical forward speed compared to the modeled 1898 TC (Fig. 26). MSLP for the modeled 2024 TC began at around 940 mb. At landfall, MSLP was just below 960 mb. The modeled 2024 storm also began rapidly weakening after landfall.

While wind speeds for the modeled 2024 TC began like the modeled 1898 storm, they decreased more rapidly beginning with a sharp decrease around 4 UTC on October 2. Furthermore, the modeled 2024 TC remained weaker than HURDAT2 records with a maximum wind speed of

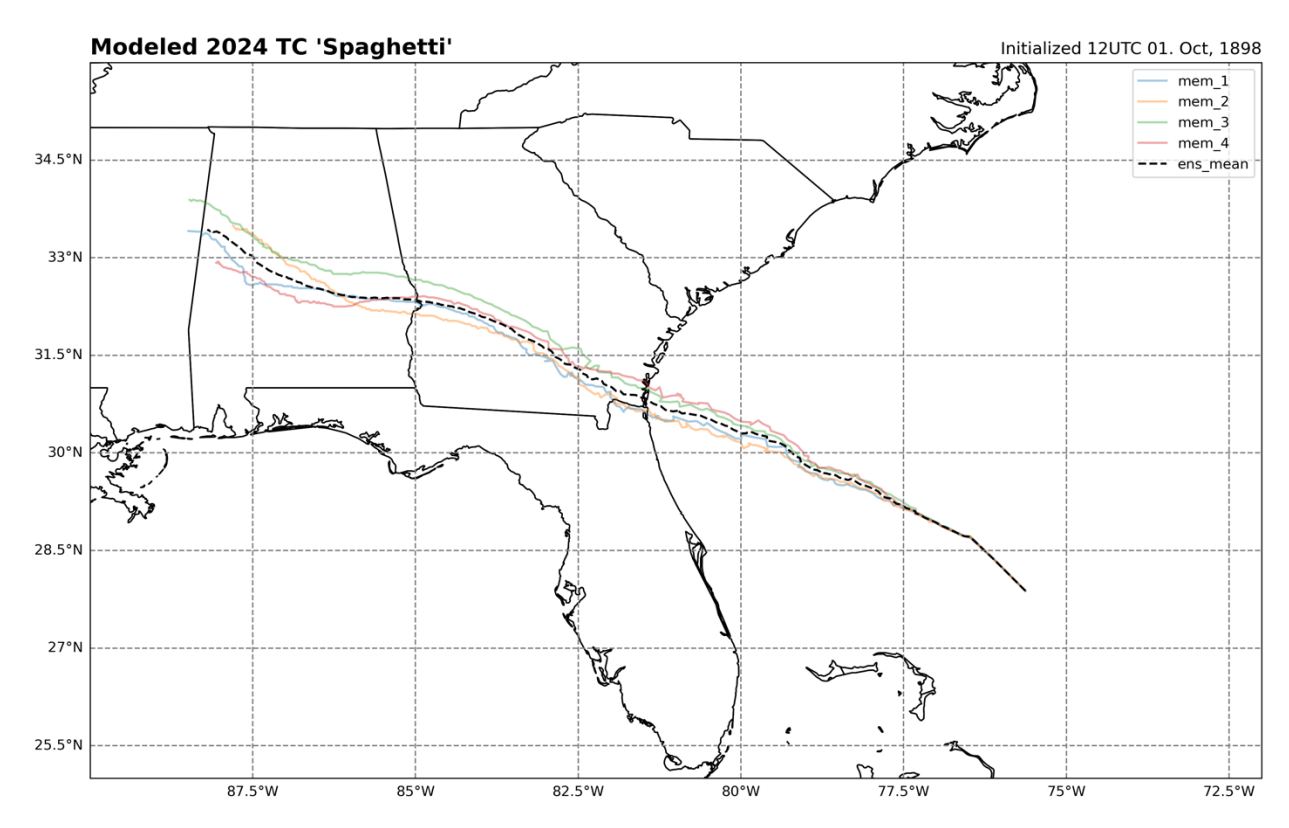


Figure 25: Tracks of the modeled mean 2024 TC and ensemble members

around 100 knots (Fig. 28). At landfall, winds in the modeled 2024 TC were around 80 knots (Fig. 28). The wind field of the modeled 2024 TC was less widespread than the modeled 1898 TC. The highest winds in the modeled 2024 TC's wind field were confined to Georgia. The strongest winds in South Carolina were limited to the south-east portion of the state. The corridor of maximum winds in Georgia was located to the north of the storm roughly between Brunswick, GA and Savannah, GA (Fig. 29).

Rainfall for the modeled 2024 TC was similar to the modeled 1898 TC. Most rainfall occurred offshore with the largest accumulations being from 6 to 8 inches. On land, rainfall was

still heaviest on the coastline with widespread accumulations up to 3 inches and isolated pockets of 4 inches. Interestingly, there was a pocket of accumulation up to 6 inches near the Brunswick, GA area in this model run. Overall, compared to the modeled 1898 TC, the area of heaviest rainfall

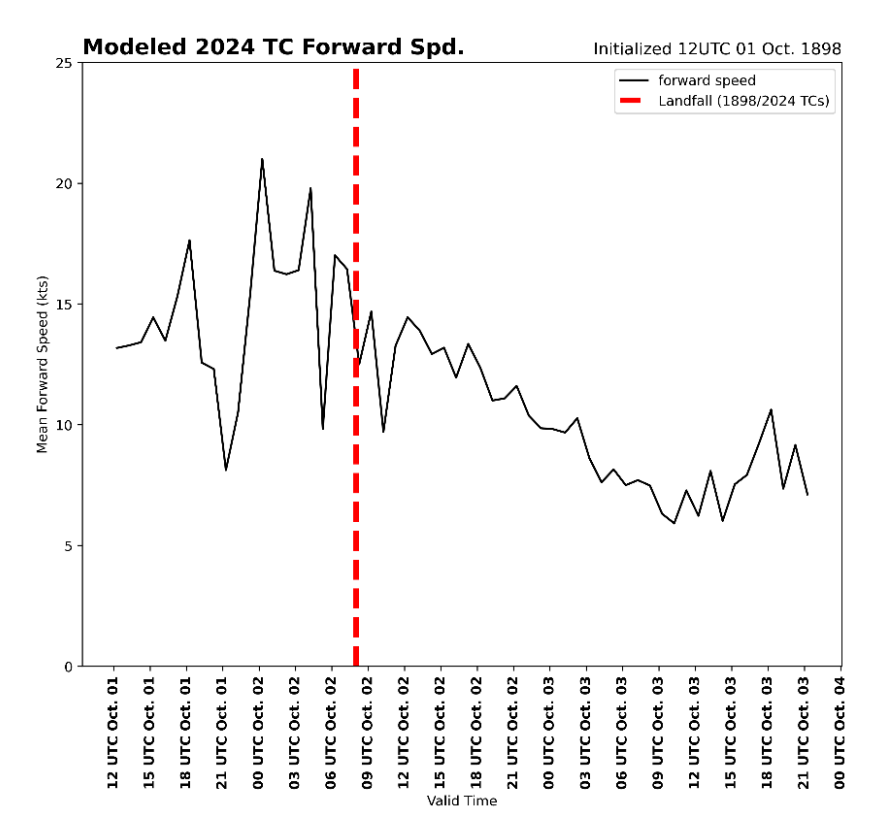


Figure 26: 2024 TC modeled MSLP (15-minute average)

seemed to be closer to land with some 6-inch accumulations extending as far west as 81.7°W (Fig. 30). This is much further west than the modeled 1898 TC's 6-inch accumulation which only extended to around 81.0°W (see Fig. 19).

The lowest landfalling pressures for the modeled 2024 TC were in Brunswick and Jacksonville at around 968 mb (Fig. 31 A, B). In Savannah and Charleston pressures were much higher at 988 mb and 998 mb, respectively (Fig. 31 C, D). Compared to the modeled 1898 storm, pressures were higher in every city except Jacksonville (see Fig. 20). This might be related to 2 of

the simulated TC's in this run that passed almost directly over Jacksonville (the mean track for the modeled 2024 TC appears to be slightly south of the modeled 1898 TC, see Fig. 14). Wind speeds at 10 meters were derived from points located just as with the modeled 1898 TC (see location of points in Fig. 21). Across all 4 cities, the 10-meter winds were nearly identical in strength to the modeled 1898 TC (Fig. 32).

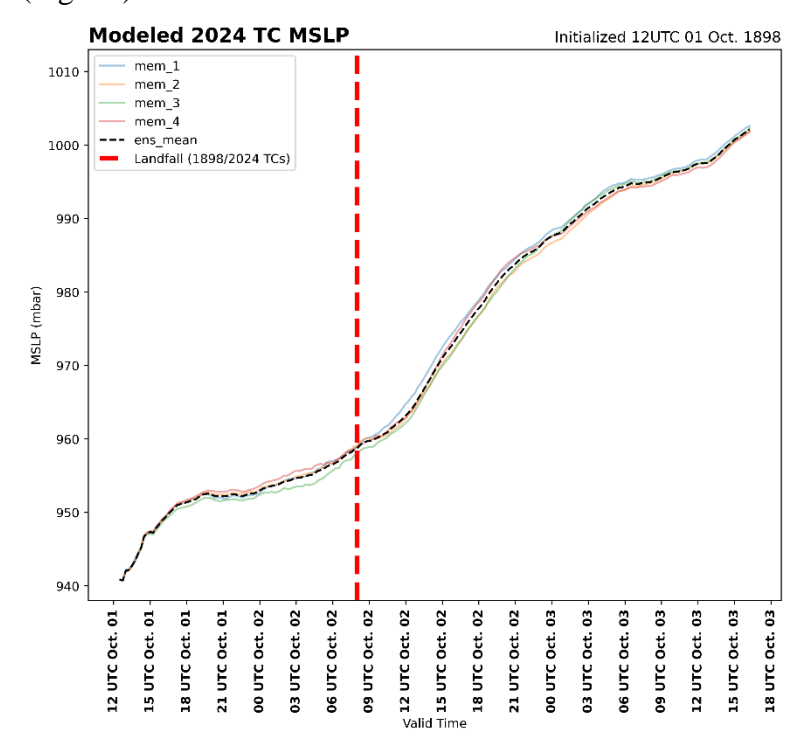
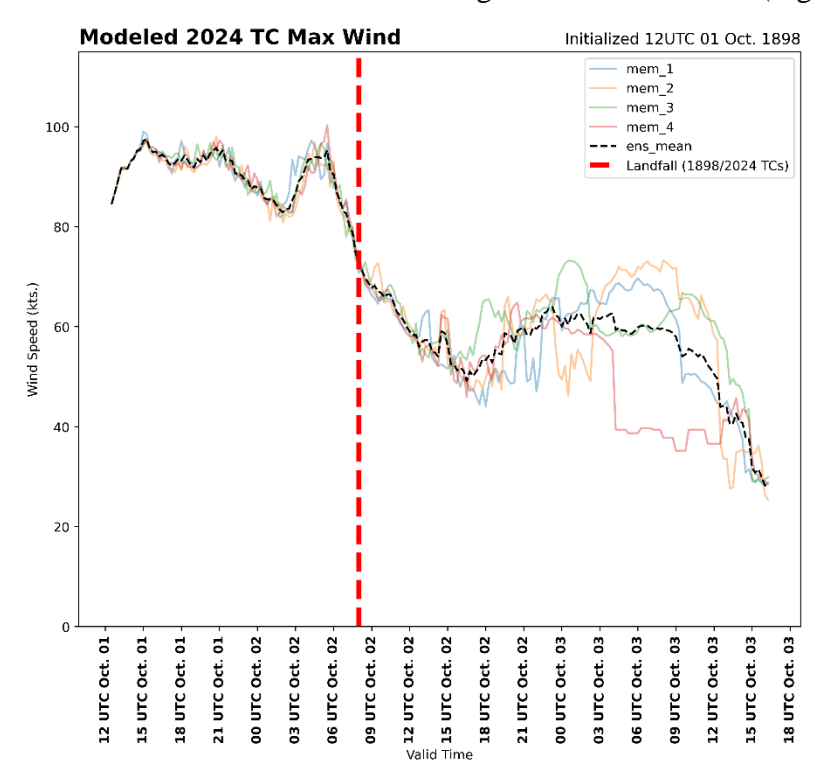


Figure 27: 2024 TC modeled MSLP (15-minute average)

Modeled storm surge for the 2024 TC is largely unchanged from the modeled 1898 TC outside of the location of maximum surge. This is not unexpected as the two main variables considered by SLOSH are pressure differential between the storm and its environment and radius of maximum winds. The only major difference was a slightly higher modeled surge on the barrier islands of Glynn County where surge was 16 feet NAVD and higher in some areas (Figs. 33, 34). The highest modeled surge was again on St. Simon's Island where values were at or over 16 feet

NAVD on the south-eastern and eastern portions of the island. Modeled surge propagated far inland with values between 6 and 10 feet NAVD along the Altamaha River (Fig. 34).



**Figure 28:** 2024 TC modeled maximum wind speed (15-minute average)

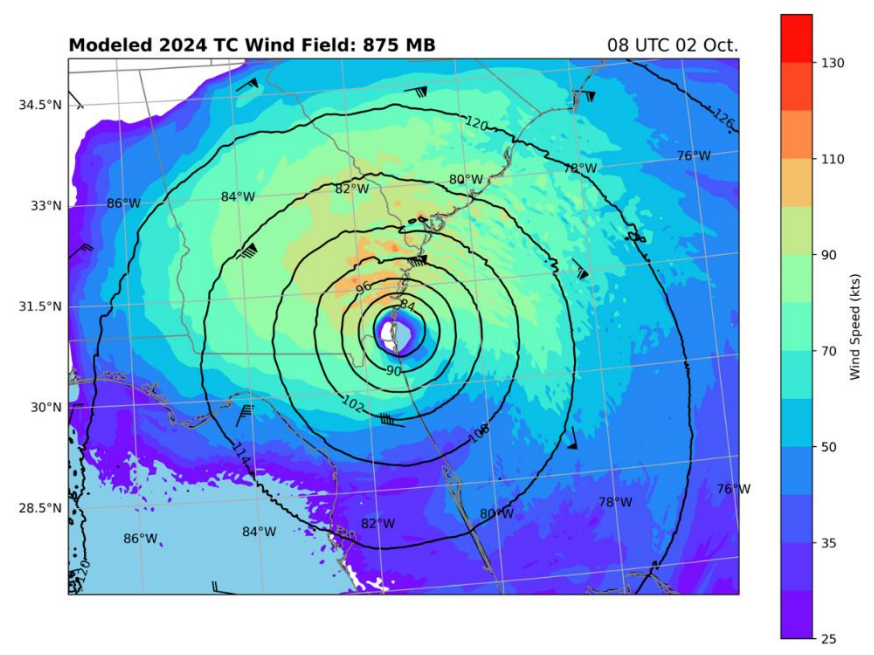
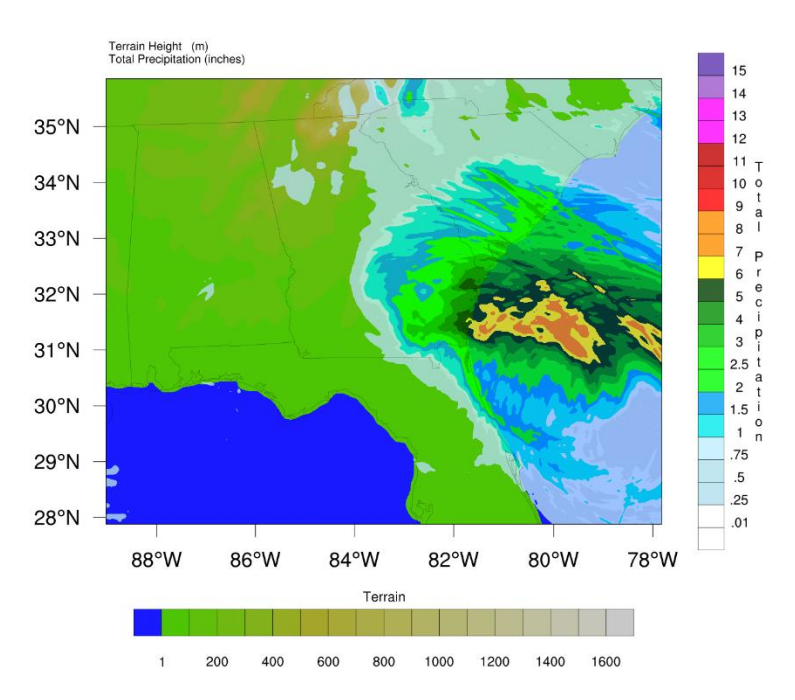


Figure 29: 2024 TC modeled wind field at landfall



**Figure 30:** 2024 TC run-total (~ 60 hours) modeled accumulated precipitation

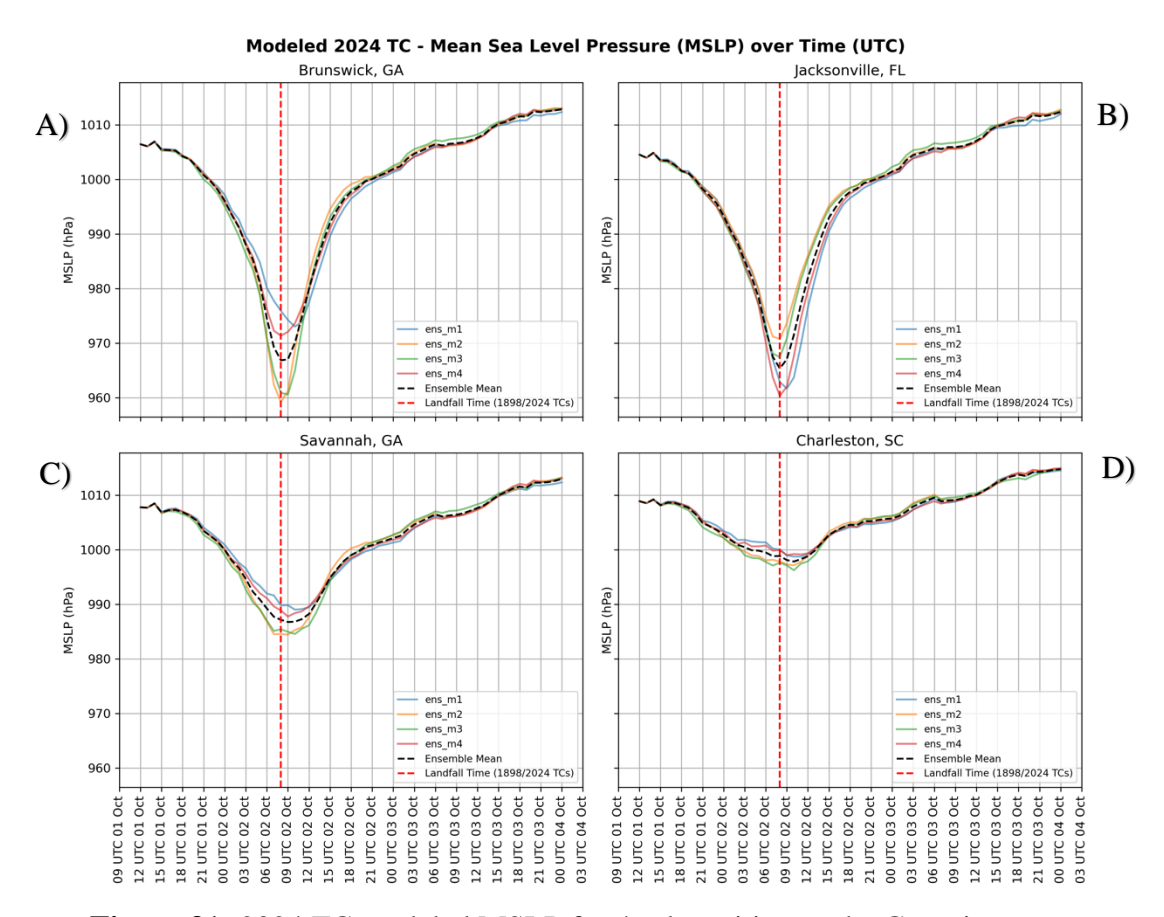
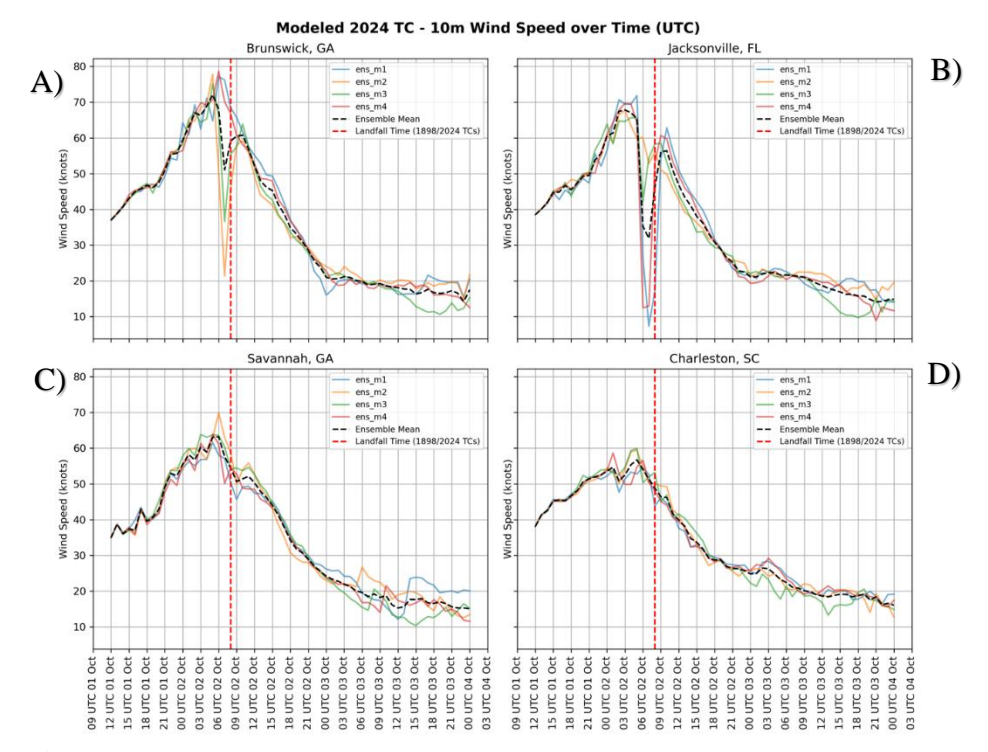


Figure 31: 2024 TC modeled MSLP for 4 select cities on the Georgia coast



**Figure 32:** 1898 Modeled TC 10m wind speeds for 4 select cities on the Georgia coast

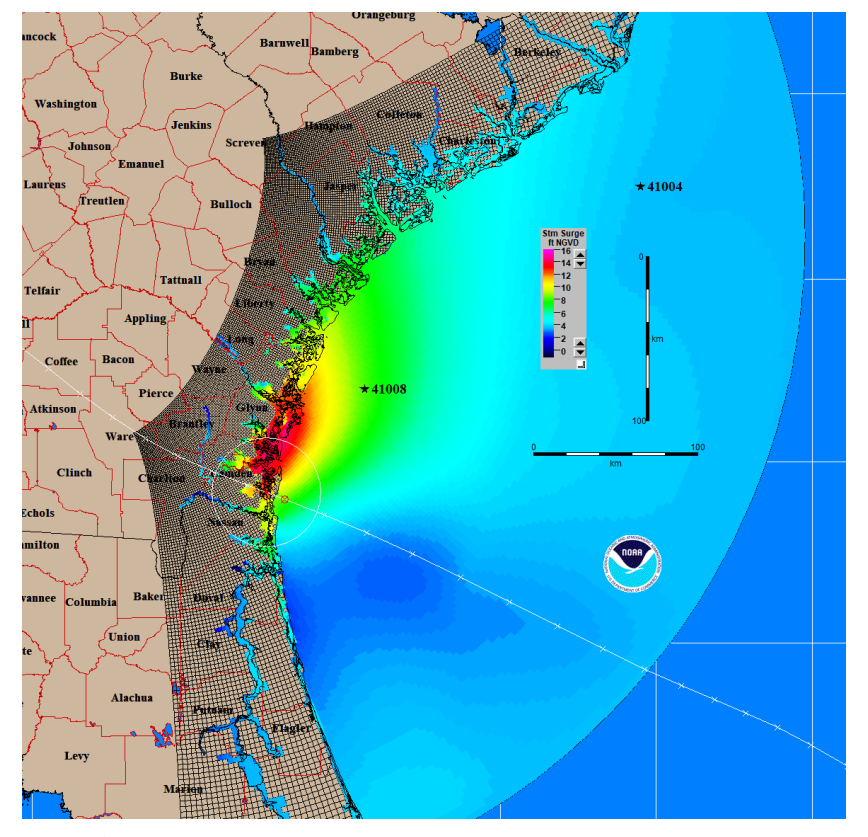
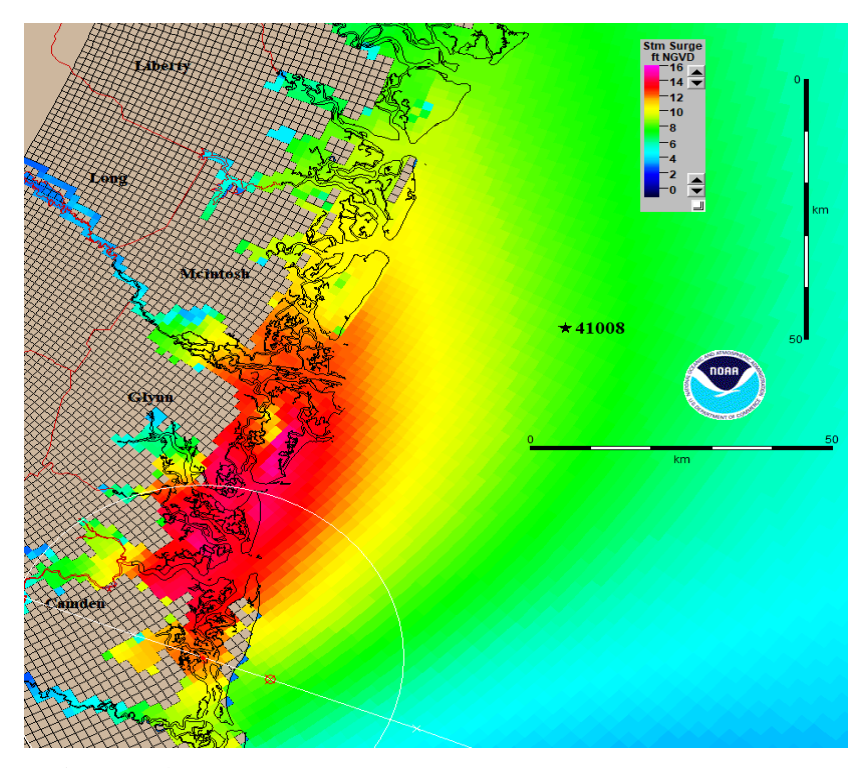


Figure 33: Overview of the modeled 2024 storm surge



**Figure 34:** Same as Fig. 33 but zoomed in on the Brunswick, GA area

## SSP 370: 1898 TC in Future Climate Conditions (2098)

The modeled 2098 TC made landfall further north across all 4 forced ensemble members. This put the landfall location much closer to the Savannah, GA area (Fig. 35). The forward speed of the modeled 2098 TC was lower than the previous two model runs, meaning the storm made landfall much later compared to the previous runs (landfall ~15 UTC 2 Oct., Fig. 36). Ensemble mean MSLP at landfall of the modeled 2098 storm was slightly higher at ~963 mb (Fig. 37). In future conditions, the storm's landfalling windspeed remains largely unchanged from the two previous runs at ~70 kts making the modeled 2098 TC a category 1 at landfall (Fig. 38). The compact wind field at landfall for the modeled 2098 TC was displaced to the west (inland) of the vortex with a much less northern extent compared to the previous model runs (Fig. 39).

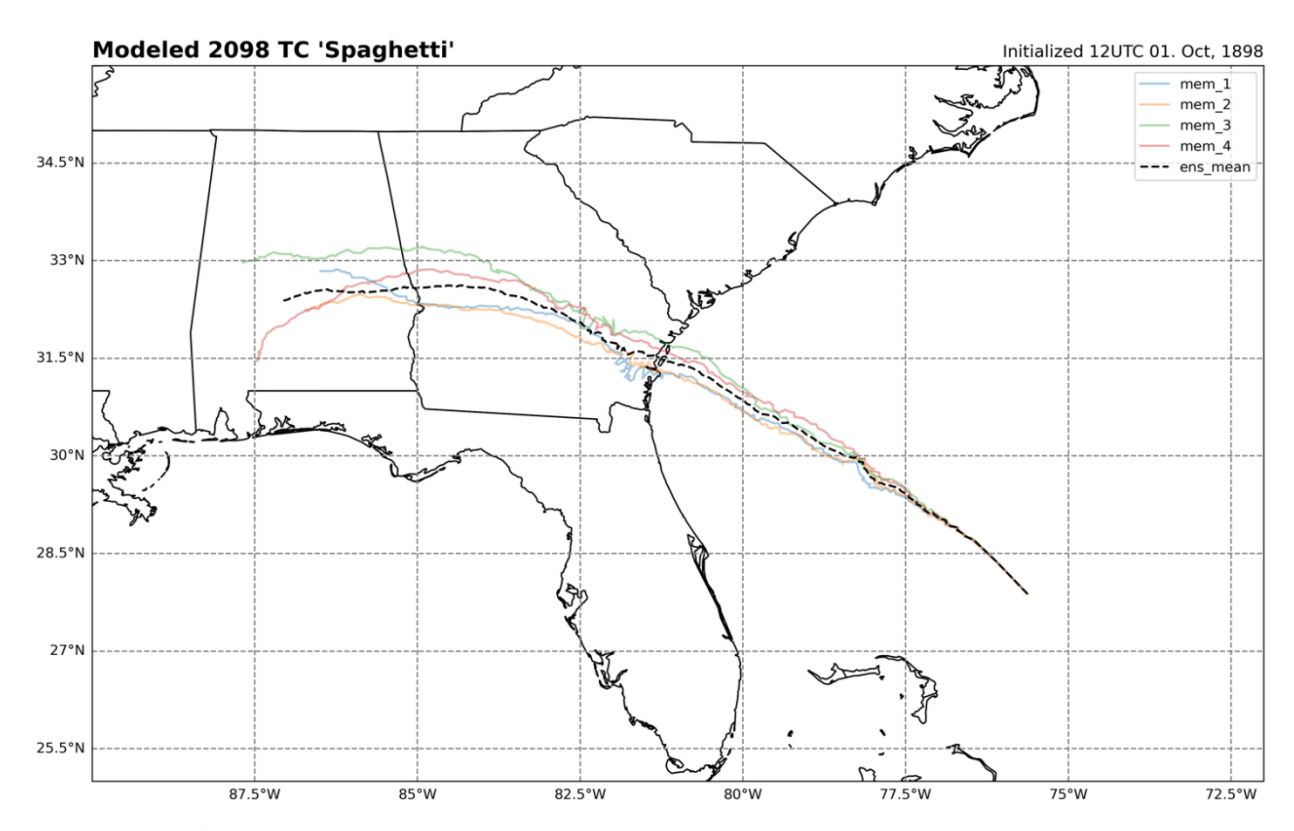


Figure 35: Tracks of the modeled mean 2098 TC and ensemble members

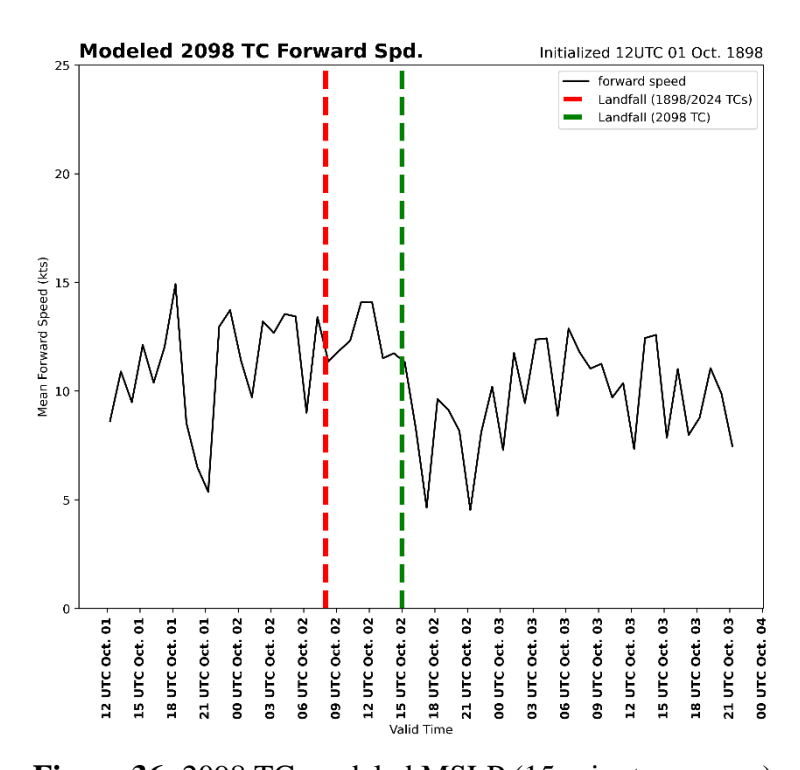


Figure 36: 2098 TC modeled MSLP (15-minute average)

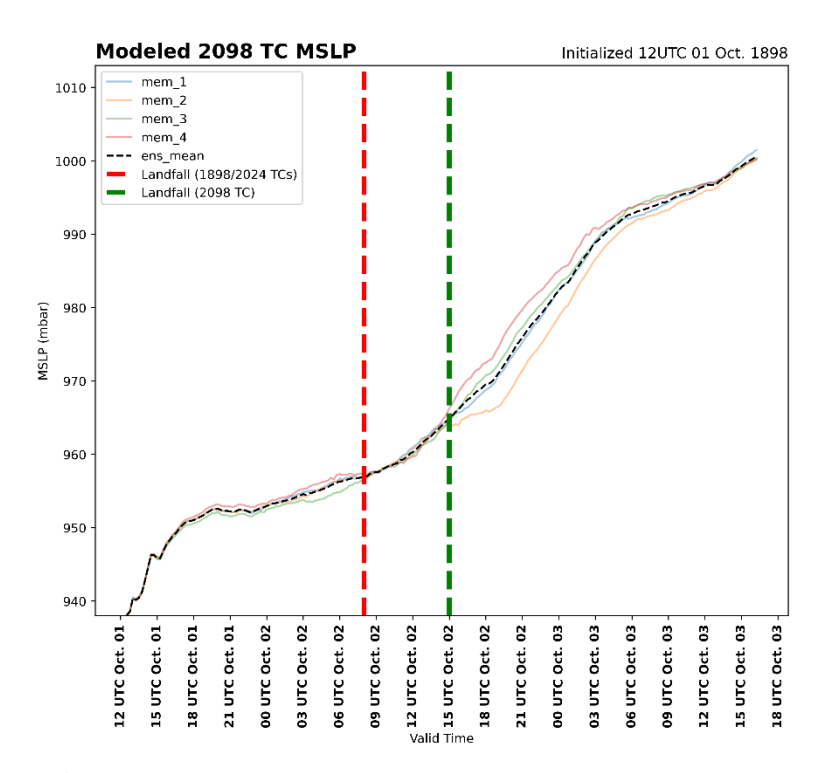
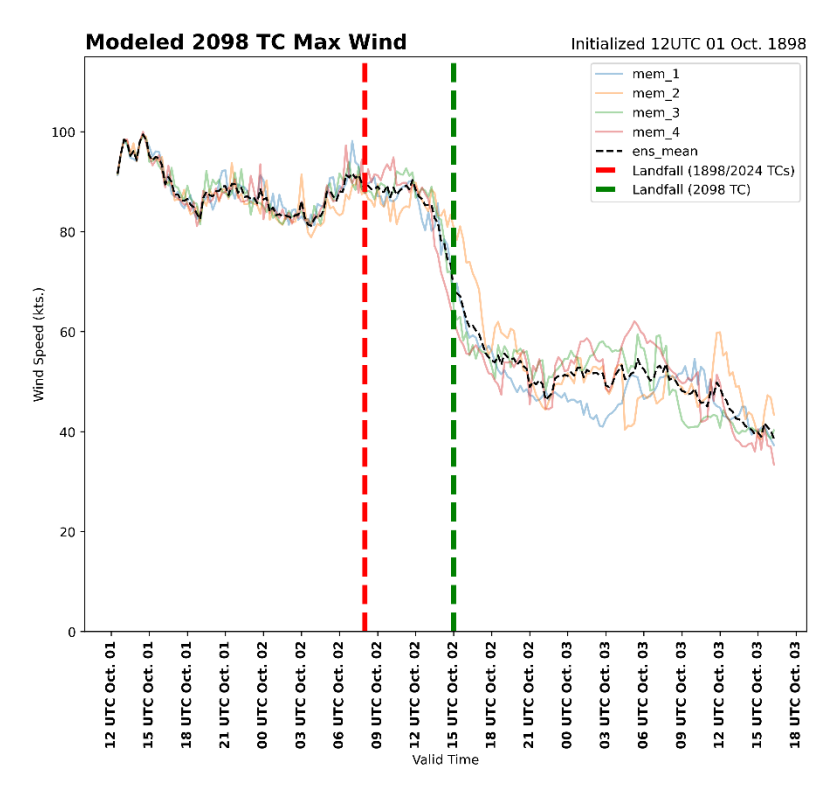


Figure 37: 2098 TC modeled MSLP (15-minute average)



**Figure 38:** 2098 TC modeled maximum wind speed (15-minute average)

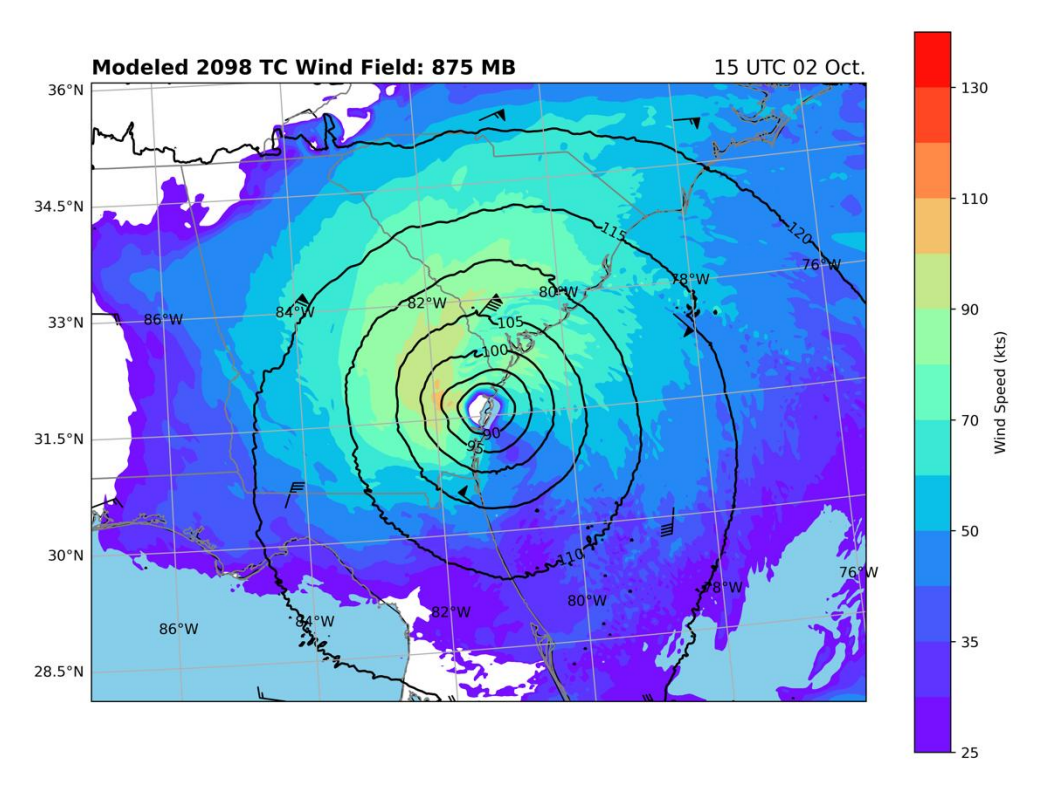
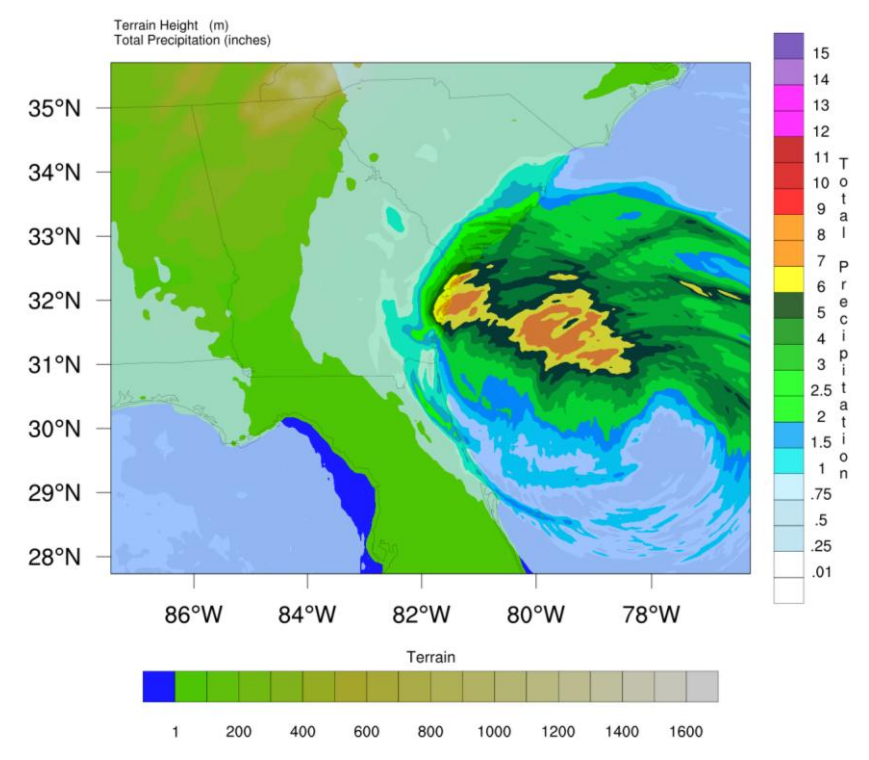


Figure 39: 2098 TC modeled wind field at landfall

The modeled 2098 TC had more rainfall accumulation than any other run, especially along the coast. The Savannah, GA area was particularly affected by increased precipitation with rainfall totals increasing from around 5 inches to 6-7 inches. South-eastern South Carolina also received much higher precipitation with the modeled 2098 TC. The slower forward speed of the modeled 2098 TC is also apparent in precipitation accumulation as less precipitation is recorded inland (Fig. 40). Across the 4 selected cities, MSLP for the modeled 2098 storm reflects the northward shift in track as Savannah and Charleston both had their lowest minimum pressures recorded during this run at 980 mb and 990 mb, respectively (Fig. 41 C, D). Brunswick and Jacksonville both had their highest minimum pressures at 975 mb and 985 mb (Fig. 41 A, B). The same northward trend from MSLP is seen in 10-meter wind speeds for the modeled 2098 TC. The highest 10-meter winds are in Brunswick at ~70 kts (Fig. 42 A). Savannah had the second highest 10m winds of the run at ~65

knots (Fig. 42 C) while Jacksonville and Charleston both had modeled 10-meter winds at ~60 kts (Fig. 42 B, D). This apparent lack of increased intensity is interesting given the 2098 climate forcings and will be discussed in later sections.



**Figure 40:** 2098 TC run-total (~ 60 hours) modeled accumulated precipitation

Modeled storm surge from SLOSH for the modeled 2098 TC was deeper than the other 2 runs an hour before landfall. The further north track also shifted the bulk of modeled surge towards the Savannah area. Further south, on Saint Catherines Island (barrier island of Liberty County, GA) modeled surge was approaching 12 feet NAVD an hour before landfall. North of this area, Tybee Island (a barrier island of Chatham County, GA) had nearly 10 feet NAVD of modeled storm surge (Fig. 43).

After landfall, the modeled 2098 TC surge is focused around the Savannah area. Saint Catherines Island had the most modeled surge approaching 16 feet NAVD. Further north, Ossabaw

Island, Skidaway Island, and Tybee Island both experienced modeled surge between 12 and 14 feet NAVD. With the modeled 2098 TC, SLOSH also showed surge moving up the Savannah River and surrounding waterways with levels of 8 feet NAVD several kilometers inland including near the city of Savannah. Heavy surge extended north and east along the coast to Charleston, SC where values were between 6 and 8 feet NAVD. The 2098 SLOSH run was marked by clear offshore flow to the south of the Brunswick, GA area associated with the westerly winds on the southern side of the TC. This flow was visible in the previous 2 runs, but the 2098 SLOSH run produced a more widespread area of offshore flow extending from the Brunswick area south down the coastline (Fig. 44).

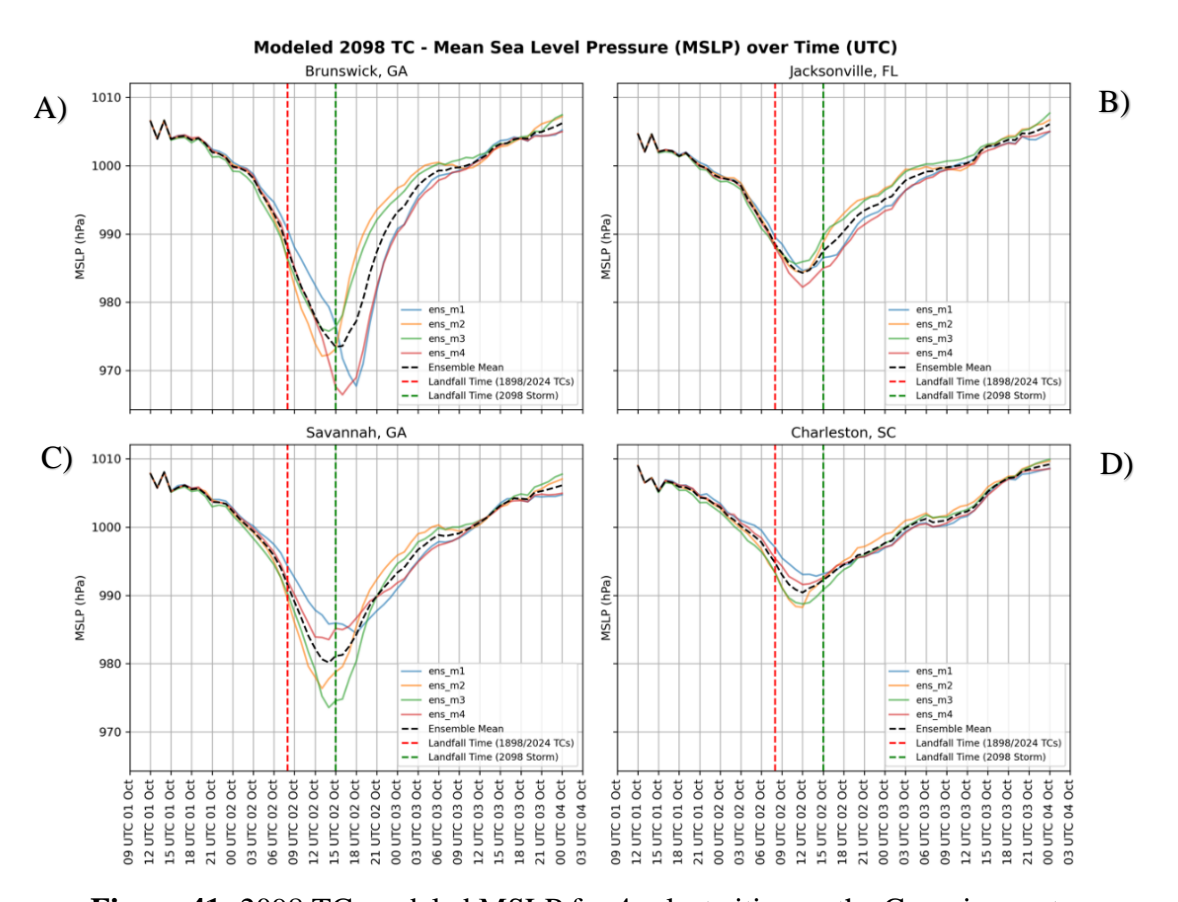
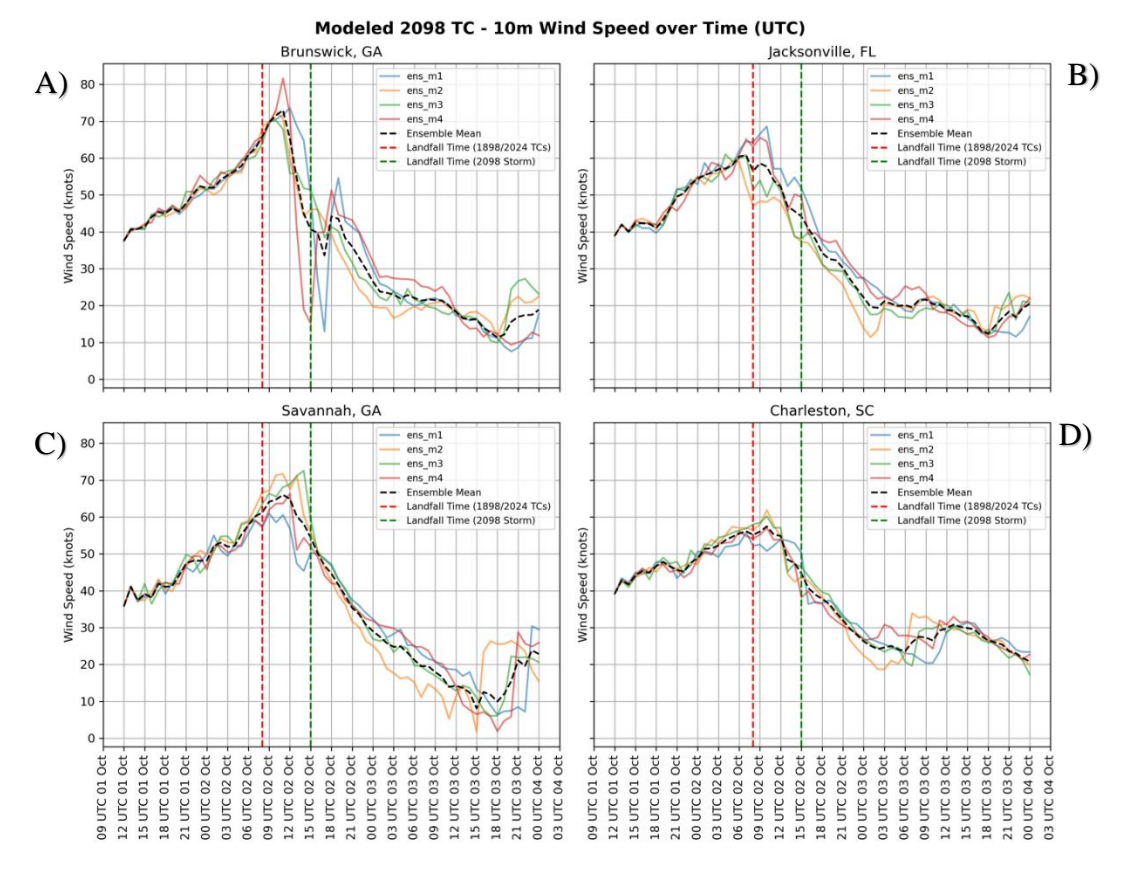


Figure 41: 2098 TC modeled MSLP for 4 select cities on the Georgia coast



**Figure 42:** 2098 Modeled TC 10m wind speeds for 4 select cities on the Georgia coast

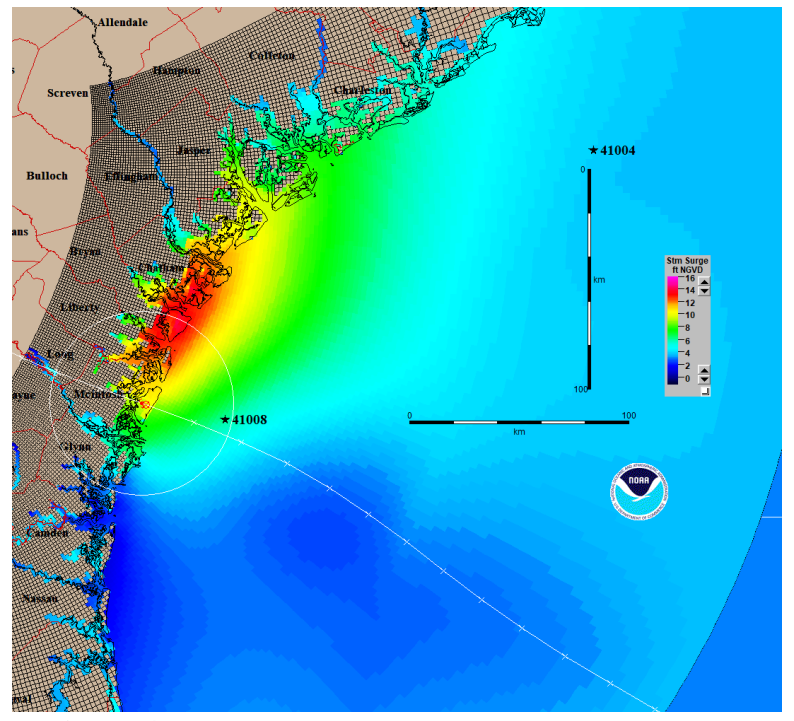
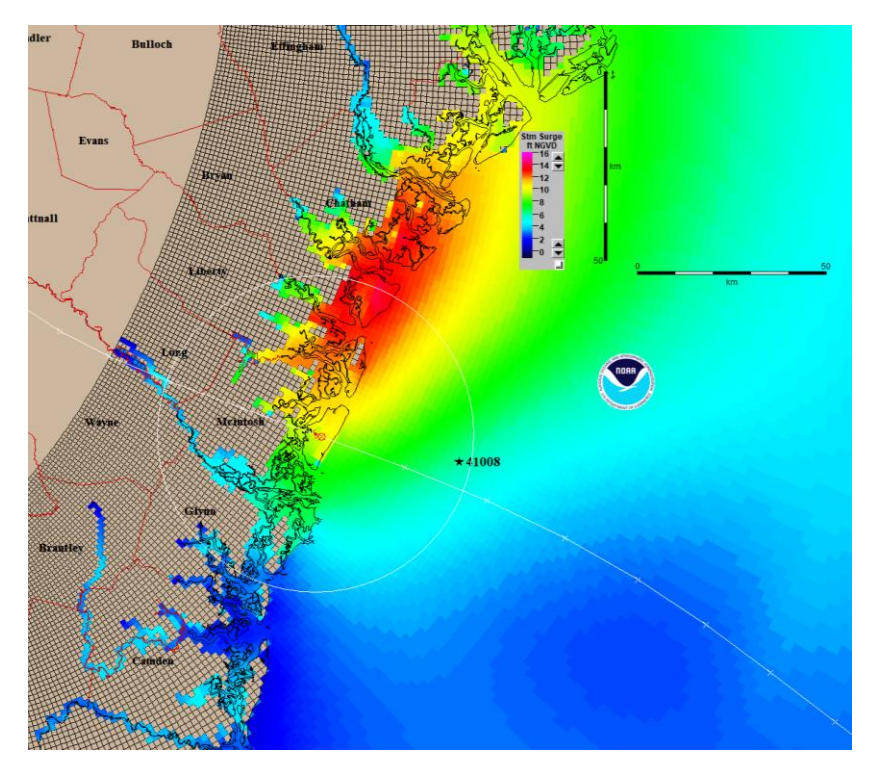


Figure 43: Overview of the modeled 2024 storm surge



**Figure 44:** Same as Fig. 43 but zoomed in on the Savannah, GA area

### **CHAPTER 5**

### DISCUSSION

### Modeled 1898 TC vs. Observed TC

The modeled 1898 TC was much weaker by wind speed in all WRF model runs of this study. While some of this difference in strength from HURDAT2 might be a result of parameterizations within the WRF model, a discussion of the observational discrepancies and sparsity regarding the late 19<sup>th</sup> century cyclone is necessary.

The modeled 1898 TC's track was nearly co-located with the sparse observations and HURDAT2. First, Sandrik and Landsea (2003) "inference" modeling using SLOSH and observed storm surge indicated the presence of a major TC, which was the original focus of this work. However, after multiple WRF model configurations were tested, a weaker storm was consistently produced. Furthermore, in the finalized 16-member ensemble output (using WRF-ARW best-practices, and the tropical parameterization suite), the storm was consistently weaker in wind speed despite following a near-identical track to the one seen in historical documents. The storm's windspeed was only mentioned 2 times in reports from the U.S. Weather Bureau (Garriott 1898).

One observed wind measurement in Savannah, GA was recorded as "60 miles per hour from the northeast at 11:30 am". The only other measurement from this document recorded winds of 60 miles per hour occurring in Jacksonville at "11 am 2d." While the modeled 1898 TC made landfall about 7 hours earlier at 8 UTC (4 AM local), it both produced landfalling modeled wind speeds sufficient to match these observations in both locations (see Fig. 22). Only one mention of potential wind damage available from in-situ observations of the storm was a Tybee Island resident's house that was "blown away" (Garriott 1898). Sand was also "piled up to 21 feet in the works" at the fort in Tybee Island. However, because these were the only explicit mention of wind

damage from the storm (the rest being flooding and storm surge), there is little observational data to concur with winds of 135 mph as mentioned in Sandrik and Landsea (2003). Furthermore, no modeled storms in this study had winds of 135 mph, even at their most intense. Given the location of the landfall being consistent in both modeling and observations, the observed winds might have also been outside of the radius of hurricane-force winds (>74 mph, >65 kts).

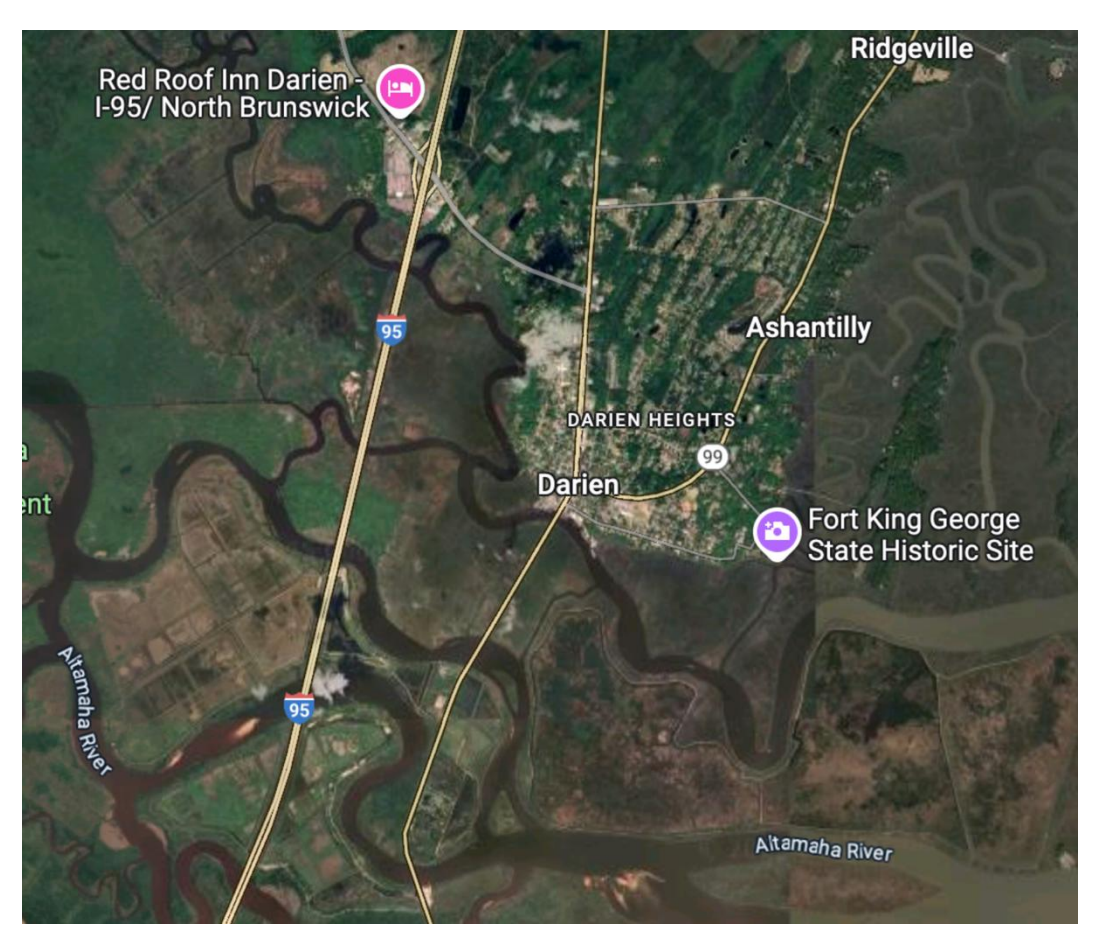


**Figure 45:** Satellite imagery of I-95 crossing the Altamaha River. Developments in Darien, GA are seen north of the river (Google Maps)

Most observed destruction was reported as the result of widespread catastrophic inundation by storm surge. The observed storm surge of the modeled storm *was* remarkably consistent with observations from 1898. There are two potential reasons that modeled surge was consistent with

observations despite weaker winds in the modeled storm. First, the limited HURDAT2 wind data shows a category 4 storm, but these winds were inferred from SLOSH and not directly modeled by a physical atmospheric model such as WRF-ARW. Secondly, SLOSH uses its own parametric wind model based entirely on pressure differential between the TC and its environment. It is possible that the statistical wind model in SLOSH was overestimating both the extent and intensity of the storm's wind. However, comparison to official NOAA storm surge maps (see Fig. 7 of Background section) shows that even a category 1 storm can produce both the surge modeled in this study and observed in 1898.

In Brunswick, GA, storm surge was observed to be "16 feet." In Darien, GA, just north of Brunswick, observed surge was 13 feet inland on the Altamaha River and 18 feet at the Sapelo Island Lighthouse (referred to as "Sapel's Lighthouse" in the document; Garriott 1898). These modeled surges are consistent with the observations above (refer to Figs. 23, 24). The surge of "16 feet" in Brunswick was cited by several other studies (including Sandrik and Landsea 2003) and enough to flood "Nearly every business house and warehouse" (Garriott 1898). Modeled surge in



**Figure 46:** An undated picture of the flooded streets of Brunswick, GA after the 1898 TC (from New Georgia Encyclopedia)

Brunswick was slightly lower than observations, but still at or above 12 feet (see Fig. 24). Furthermore, a local stated that a flood of that severity had not been seen in the area "since 1812" (Garriott 1898).

## Potential Effects of a Similar Storm Today (2025)

The population of most of the cities discussed here has only increased in the 125 years since 1898. Furthermore, increases in the infrastructure crossing the areas where the storm caused the most damage has created opportunities for even more substantial damage. One example of development is the Interstate-95 corridor that stretches along coastal Georgia and Florida. A storm surge of this magnitude (13-18 feet in some areas around Darien) would undoubtedly flood the interstate and associated bridges at a minimum. A storm with higher windspeeds might cause structural damages to the overpasses and nearby structures along the road. While the interstate is further inland than some other state and federal routes in the area, the highway travels close to the coastline, particularly in the Brunswick/Darien area. It also crosses over several waterways, one of which is the Altamaha River where upstream surge damage was explicitly mentioned in the U.S. Weather Bureau article (Garriott 1898; see Fig. 24).

Determining the integrity of structures in the area is beyond the scope of this study, but the storm surge associated with this storm would likely be devastating to all but the most well-built or elevated structures. There are modern examples of damage from extreme storm surge such as Hurricane Michael (2018) in Mexico Beach, Florida, or Hurricane Katrina (2005) in New Orleans, LA. Michael produced surge of 9-14 feet in Mexico Beach, while Katrina produced surge up to 28 feet in some areas (U.S. NHC 2022). While these storms may have been stronger in wind speed as well (particularly Michael, which was a category 5 with 161 mph winds at landfall), they both produced surge like the modeled and observed surge from the 1898 storm. The area of study,

which has not been directly impacted by a tropical cyclone in most residents' lifetimes, is almost certainly a hotspot of "hurricane amnesia," or even the assumption by residents of the area that such an event could not happen to them. A similar phenomenon, "disaster fatigue," arises after multiple back-to-back disasters. Despite different causes, these phenomena both impact the resilience of impacted communities negatively and can build a sense of complacency with the damage and loss coincident with disasters such as TCs (National Academies 2024). Michael and Katrina both struck in areas impacted by much more recently landfalling storms still to catastrophic results. Sea-level rise, a well-documented consequence of climate change, will likely only serve to exacerbate the surge in these areas. As such, it should be noted that the surge modeling in this study used mean sea levels from 1929.

Regardless of certainty in the surface metrics of the 1898 TC, there are several small coastal cities in Georgia similar to Mexico Beach, FL (i.e. Fig. 2, discussed in Background). Tybee Island is an example of one such city, but many coastal Georgia cities are small like Mexico Beach, FL. If the winds and surge associated with this storm impacted Tybee Island today, the scene might be like that of Mexico Beach after Hurricane Michael.

### Some Impacts of Future Climate Forcing on the 1898 TC

Climate change has altered weather events worldwide in recent years, including tropical cyclones. Phenomena such as rapid intensification coupled with hyperactive hurricane seasons have produced near consistent record-breaking storm seasons, especially in the 2020s. For the modeled 1898 storm, present-day (2024) and future (2098) climate forcings from CESM2-LENS produced storms with similar winds and pressure. The modeled 2024 TC was largely unchanged from the modeled 1898 TC in track, wind, and pressure. Modeled storm surge for this TC was also similar. The modeled 2098 TC was a slower-moving storm on average (see Fig. 38), and one that

produced higher rainfall amounts, particularly in coastal areas (see Fig. 42). Recent literature suggests that, in a warmer climate, TCs may slow down, although this claim is still subject to debate (Kossin 2018). Furthermore, the modeled surge for the modeled 2098 TC was much further north and impacted the Savannah, GA area more than any other storm. Overall, an 1898 Georgia TC forced by 2098 climate conditions produced a slower-moving and wetter storm with similar conditions.

### **Important Considerations for this Modeling Study**

While most of the uncertainty in this study is attributed to lack of observations from the time of the storm, there are other uncertainties within WRF-ARW, particularly with intensity. While TC track forecasting accuracy has increased significantly over the last few decades, intensity forecasting remains a challenge even for bleeding-edge models. As such, the intensity of the storm in this study is not certain. The Sandrik and Landsea (2003) storm from SLOSH was determined to have maximum winds of 135 mph making the 1898 TC a category 4 major hurricane. However, there are no records of a storm of that strength at landfall. Most damage mentioned by the U.S. Weather Bureau was from storm surge.

Furthermore, upon examining SLOSH model output from NOAA's version 3 Storm Surge maps website, a category 1 storm like the one in this study produces a surge greater than 9 feet across the Brunswick/Darien, GA area (see Fig. 4). A major hurricane does *not* appear to be necessary to create the surge intensity recorded in 1898 observations, or in this modeling study. While updated surge maps have undoubtedly offered better insight into surge across US coastal basins, the Sandrik and Landsea (2003) study's category 4 storm is not necessary to obtain recorded results (according to NOAA's SLOSH model). Sandrik and Landsea (2003) has also become a prolific source of online information on this storm which might explain in part why it is

often noted as category 4 despite few recorded observations of windspeed. A modern-day storm making landfall in this area would be the only way to quantify the impacts with certainty, but this has not happened since 1898.

One final point regarding the surge modeling in this study was the lack of consideration of sea level rise. It is known that global sea levels will rise with a warming climate over the next century (NOAA 2023). Sea level rise is already impacting some coastal areas. This study utilized 1929 sea levels to model storm surge. It is likely that the surge seen in this study is an *underestimation*, especially when considering the present-day and future timeframes. Future work considering a historical storm in future environments might consider accounting for this background rise in sea level to obtain the most accurate modeling of storm surge, regardless of the storm surge model used.

## **Lack of Certainty in Surface Wind Speeds**

To quantify surface wind effects in this study, winds just offshore of cities of interest were used instead of the exact geographic center of the cities. One reason why was that, when comparing winds at the 875 hPa pressure surface to 10m winds from WRF-ARW output, the resulting difference seems unrealistic. For example, the 875 mb winds just offshore the Brunswick, GA area were modeled over 110 kts. in original, present-day, and future runs. In several timesteps, simultaneously calculated 10m winds were only around 30 knots (Fig. 47). Furthermore, comparisons between surface pressure and calculated 10m wind plots for multiple cities also seemed unrealistic. At one point (close to landfall in the model), the SLP in Brunswick falls to ~958 mb while surface winds barely reach 34 kts.

Further bolstering the decision to prefer co-located but offshore winds wind is the stark gradient in wind speed from open ocean to land. While it is a well-known fact that winds over land

will slow because of friction (this is a component of the death of TCs), the modeled 10m winds seemed unphysical. There were even some instances where the winds slowed even before contacting land. The inaccuracy of low-level wind modeling in WRF is documented in some literature. Of important note is the complex terrain and biases introduced from the synoptic scale flow patterns (Jimenez et al. 2013). Furthermore, the accurate description of seasonal changes in land cover and land type might play a role in low level wind calculations (Duan et al. 2018). Under guidance from literature and given the inherent uncertainty in conditions from the late 19th century (including a lack of reliable observations to verify model output) the decision was made to remove complicating factors such as high-resolution terrain. The vortex-following software native to WRF-ARW used for some of the figures in this study is also much different in wind speed, even after landfall.

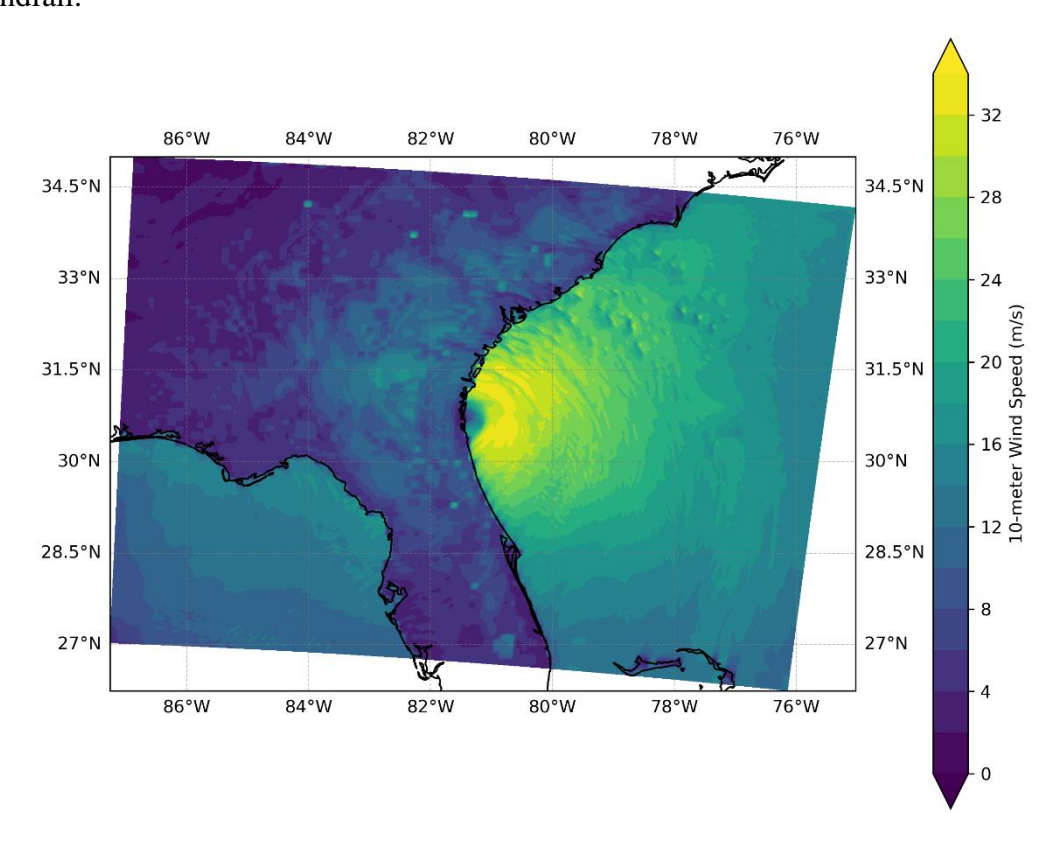


**Figure 47:** An example of 10m wind speed showing a stark contrast between land and ocean, especially along the northeast Florida coast

### CHAPTER 6

### CONCLUSIONS AND FUTURE WORK

This modeling study employed WRF-ARW to downscale reanalysis data from the NOAA/DOE 20<sup>th</sup> Century Reanalysis version 3 (20CRv3) dataset to model some impacts associated with the last tropical cyclone to make landfall in coastal Georgia. Furthermore, the study also coupled NOAA's SLOSH model to the modeled storm to analyze the extent of the storm surge produced by the modeled storm. CESM2-LENS climate data was used to force WRF-ARW simulations towards present-day (2024) and future (2098) climate conditions to investigate any major impacts on storm path or intensity if the 1898 TC were to happen today, or in the future, 200 years after its original occurrence.

While there are several assumptions made within the modeling of this study, the uncertainty of initial conditions in the 19<sup>th</sup> century (a result of the lack of observations) leaves reanalysis of this storm to records in newspapers and by reports from locals. There are also potential errors in both reporting (misspellings, wrong dates, wrong times, etc.) and in measurements.

This study revealed a few key points for consideration in future work involving this storm. First, the 1898 Georgia Hurricane may *not* have been as strong as previously recorded. Available records, despite their sparseness, did not indicate a storm of category 4 strength such as the one in Sandrik and Landsea (2003). Furthermore, the WRF-ARW struggled to produce a weak category 3 storm even at sea with minimal impacts from land. Model output, including surge and MSLP indicate a modeled storm close to the few in-situ observations available for the storm.

Secondly, if the 1898 Georgia TC was transferred into a 2098 climate, 200 years later, it would potentially be a wetter storm (especially on land) with similar sustained wind speeds. There

is also evidence to suggest that, in 2098 conditions, the Georgia TC would have had a slower forward speed than the original 1898 storm. Finally, a major hurricane may not be a requirement for catastrophic storm surge on the Georgia coast. Even though the 1898 TC was a category 1 storm at landfall in the unforced runs, it produced catastrophic modeled storm surge all along the Georgia coastline. In-situ observations correspond with the extent of the damage of this study, regardless of the strength of the modeled TC.

Future studies might seek to use more recent models moving forward as WRF-ARW and HWRF are no longer actively supported by NCAR. Newer models, such as HMON and the successor to WRF, MPAS, have shown promising results on continuing to improve TC intensity forecasting in an increasingly changing climate. Furthermore, as reanalysis modeling improves, this study could be run with more accuracy. Lastly, newer methodologies and models for predicting challenging phenomena such as rapid intensification will be paramount to the future modeling of TCs in an ever-changing climate.

### REFERENCES

- Berner, J., G. J. Shutts, M. Leutbecher, and T. N. Palmer, 2009: A spectral stochastic kinetic energy backscatter scheme and its impact on flow-dependent predictability in the ECMWF ensemble prediction system. *J. Atmos. Sci.*, **66**, 603–626.
- Berner, J., K. R. Fossell, S. Ha, J. P. Hacker, and C. Snyder, 2015: Increasing the Skill of Probabilistic Forecasts: Understanding Performance Improvements from Model-Error Representations. *Mon. Wea. Rev.*, **143**, 1295–1320, <a href="https://doi.org/10.1175/MWR-D-14-00091.1">https://doi.org/10.1175/MWR-D-14-00091.1</a>.
- Bossak, B. H., S. S. Keihany, M. R. Welford, and E. J. Gibney, 2014: Coastal Georgia is not immune: Hurricane History, 1851–2012. *Southeastern Geographer*, **54**, 323–333, doi:10.1353/sgo.2014.0027.
- Brogli, R., C. Heim, J. Mensch, S. L. Sørland, and C. Schär, 2023: The pseudo-global-warming (PGW) approach: Methodology, software package PGW4ERA5 v1.1, validation, and sensitivity analyses. *Geosci. Model Dev.*, **16**, 907–926, <a href="https://doi.org/10.5194/gmd-16-907-2023">https://doi.org/10.5194/gmd-16-907-2023</a>.
- Chen, F., and J. Dudhia, 2001: Coupling an advanced land-surface/ hydrology model with the Penn State/ NCAR MM5 modeling system. Part I: Model description and implementation. *Mon. Wea. Rev.*, 129, 569–585.
- Chow, T. N., C. Y. Tam, J. Chen, and C. Hu, 2024: Effects of Background Synoptic

  Environment in Controlling South China Sea Tropical Cyclone Intensity and Size Changes

- in Pseudo–Global Warming Experiments. *J. Climate*, **37**, 1811–1832, https://doi.org/10.1175/JCLI-D-23-0503.1.
- Corkran, R. T., 2024: Geospatial Analysis of Historical Tropical Cyclone Intensity and Rainfall in Georgia, United States. M.S thesis, Louisiana State University, 31315800, 3110356072, ProQuest Dissertations & Theses Global.
- Duan, H., Y. Li, T. Zhang, and Coauthors, 2018: Evaluation of the Forecast Accuracy of Near-Surface Temperature and Wind in Northwest China Based on the WRF Model. *J Meteorol Res*, **32**, 469–490. https://doi.org/10.1007/s13351-018-7115-9
- Emanuel, K. A., 2021: Atlantic tropical cyclones downscaled from climate reanalyses show increasing activity over past 150 years. *Nature Communications*, **12**, doi:10.1038/s41467-021-27364-8.
- EPA, 2023: Climate Change Indicators: Sea Surface Temperature. [Available online at <a href="https://www.epa.gov/climate-indicators/climate-change-indicators-sea-surface-temperature">https://www.epa.gov/climate-indicators/climate-change-indicators-sea-surface-temperature</a>. Accessed 2 August 2023.]
- Evans, C., R. S. Schumacher, and T. J. Galarneau, 2011: Sensitivity in the Overland Reintensification of Tropical Cyclone Erin (2007) to Near-Surface Soil Moisture Characteristics. *Mon. Wea. Rev.*, **139**, 3848–3870, <a href="https://doi.org/10.1175/2011MWR3593.1">https://doi.org/10.1175/2011MWR3593.1</a>.

- Garriott, E. B., 1898: October 1898 Monthly Weather Review, National Oceanic and Atmospheric Administration. [Available online at <a href="https://www.aoml.noaa.gov/hrd/hurdat/mwr\_pdf/1898.pdf">https://www.aoml.noaa.gov/hrd/hurdat/mwr\_pdf/1898.pdf</a>. Accessed 26 March 2025.]
- GEMA, 2022: Georgia Disaster History. [Available online at gema.georgia.gov/Georgia-disaster-history. Accessed 26 March 2025]
- Gutmann, E. D., and Coauthors, 2018: Changes in Hurricanes from a 13-Yr Convection-Permitting Pseudo–Global Warming Simulation. *J. Climate*, **31**, 3643–3657, <a href="https://doi.org/10.1175/JCLI-D-17-0391.1">https://doi.org/10.1175/JCLI-D-17-0391.1</a>.
- Hart, R. E., 2010: Simulation of historical hurricane events using 20th century reanalysis. 29th Conference on Hurricanes and Tropical Meteorology. [Available online at <a href="https://ams.confex.com/ams/29Hurricanes/techprogram/paper\_169111.html">https://ams.confex.com/ams/29Hurricanes/techprogram/paper\_169111.html</a>. Accessed 1

  August 2023.]
- Hill, K. A., and G. M. Lackmann, 2009: Analysis of Idealized Tropical Cyclone Simulations
  Using the Weather Research and Forecasting Model: Sensitivity to Turbulence
  Parameterization and Grid Spacing. *Mon. Wea. Rev.*, **137**, 745–
  765, <a href="https://doi.org/10.1175/2008MWR2220.1">https://doi.org/10.1175/2008MWR2220.1</a>.
- Hong, S. Y., and J. O. Lim, 2006: The WRF Single-Moment 6-Class Microphysics Scheme (WSM6), *J. Korean Meteor. Soc.*, 42, 129–151.
- Hong, S. Y., 2007: Stable Boundary Layer Mixing in a Vertical Diffusion Scheme. [Available online at <a href="https://ams.confex.com/ams/pdfpapers/140120.pdf">https://ams.confex.com/ams/pdfpapers/140120.pdf</a>. Accessed 14 April 2025.]

- Federal Highway Administration, 2024: National Bridge Inventory. [Available online at <a href="https://www.arcgis.com/home/item.html?id=bd1b6ee967134ea68fac351cef461b5e">https://www.arcgis.com/home/item.html?id=bd1b6ee967134ea68fac351cef461b5e</a>. Accessed 13 April 2025.]
- Hutson, A., A. Fujisaki-Manome, and B. Lofgren, 2024: Testing the Sensitivity of a WRF-Based Great Lakes Regional Climate Model to Cumulus Parameterization and Spectral Nudging. *J. Hydrometeor.*, **25**, 1007–1025, https://doi.org/10.1175/JHM-D-22-0234.1.
- Jelesnianski, C. P., J. Chen, and W. A. Shaffer, 1992: SLOSH: Sea, Lake, and Overland Surges from Hurricanes. NOAA Technical Report NWS 48, National Weather Service, 71 pp.
- Jiménez, P. A., J. Dudhia, J. F. González-Rouco, J. P. Montávez, E. García-Bustamante, J. Navarro, J. Vilà-Guerau de Arellano, and A. Muñoz-Roldán, 2013: An evaluation of WRF's ability to reproduce the surface wind over complex terrain based on typical circulation patterns, *J. Geophys. Res. Atmos.*, 118, 7651–7669, doi:10.1002/jgrd.50585.
- Knutson, T., and Coauthors, 2020: Tropical Cyclones and Climate Change Assessment: Part II: Projected Response to Anthropogenic Warming. *Bull. Amer. Meteor. Soc.*, **101**, E303–E322, <a href="https://doi.org/10.1175/BAMS-D-18-0194.1">https://doi.org/10.1175/BAMS-D-18-0194.1</a>.
- Kurihara, Y., R. E. Tuleya, and M. A. Bender, 1998: The GFDL Hurricane Prediction System and Its Performance in the 1995 Hurricane Season. *Mon. Wea. Rev.*, **126**, 1306–1322, https://doi.org/10.1175/1520-0493(1998)126<1306:TGHPSA>2.0.CO;2.

- Lackmann, G. M., 2015: Hurricane Sandy before 1900 and after 2100. *Bull. Amer. Meteor.*Soc., 96, 547–560, <a href="https://doi.org/10.1175/BAMS-D-14-00123.1">https://doi.org/10.1175/BAMS-D-14-00123.1</a>.
- Landsea, C. W., 2009: Documentation of Atlantic Tropical Cyclone Changes in HURDAT.

  National Oceanic and Atmospheric Administration, [Available online at

  https://ams.confex.com/ams/99annual/abstracts/265.html. Accessed 2 August 2023.]
- Li, G., M. Curcic, M. Iskandarani, S. S. Chen, and O. M. Knio, 2019: Uncertainty Propagation in Coupled Atmosphere–Wave–Ocean Prediction System: A Study of Hurricane Earl (2010). *Mon. Wea. Rev.*, **147**, 221–245, <a href="https://doi.org/10.1175/MWR-D-17-0371.1">https://doi.org/10.1175/MWR-D-17-0371.1</a>.
- Liu, P., A. P. Tsimpidi, Y. Hu, B. Stone, A. G. Russell, and A. Nenes, 2012: Differences between downscaling with spectral and grid nudging using WRF. *Atmos. Chem. Phys.*, **12**, 3601-3610, doi:10.5194/acp-12-3601-2012.
- Michaelis, A. C., and G. M. Lackmann, 2013: Numerical modeling of a historic storm: Simulating the blizzard of 1888. *Geophysical Research Letters*, **40**, 4092–4097. doi:10.1002/grl.50750.
- National Academies of Sciences, Engineering, and Medicine, 2024: Compounding Disasters in Gulf Coast Communities 2020-2021: Impacts, Findings, and Lessons Learned.

  Washington, DC: The National Academies Press. https://doi.org/10.17226/27170.
- National Hurricane Center, 2022: Storm Surge Risk Maps. [Available online at https://www.nhc.noaa.gov/nationalsurge/. Accessed 2 August 2023.]

- National Weather Service, 2022: Hurricane Katrina 2005. [Available online at <a href="https://www.weather.gov/mob/katrina">https://www.weather.gov/mob/katrina</a>. Accessed 13 April 2025]
- National Weather Service, 2022, Hurricane Michael 2018. [Available online at <a href="https://www.weather.gov/tae/hurricanemichael2018">https://www.weather.gov/tae/hurricanemichael2018</a>. Accessed 13 April 2025]
- NOAA, 2023: Tropical cyclone hazards. [Available online at <a href="https://www.noaa.gov/jetstream/tc-hazards">https://www.noaa.gov/jetstream/tc-hazards</a>. Accessed 2 August 2023.]
- NOAA, 2023: Climate Change: Global Sea Level. [Available online at <a href="https://www.climate.gov/news-features/understanding-climate/climate-change-global-sea-level">https://www.climate.gov/news-features/understanding-climate/climate-change-global-sea-level</a>. Accessed 14 April 2025.]
- O'Neill, B. C., E. Kriegler, K. L. Ebi, E. Kemp-Benedict, K. Riahi, D. S. Rothman, and W. Solecki, 2017: The roads ahead: Narratives for shared socioeconomic pathways describing world futures in the 21st century. *Global Environ. Change*, **42**, 169–180
- Sandrik, A., 1998: A Reevaluation of the Georgia and Northeast Florida Hurricane of 2 October 1898 Using Historical Resources. [Available online at <a href="http://www.srh.noaa.gov/jax/research/hurricanes/history/1898/index.html">http://www.srh.noaa.gov/jax/research/hurricanes/history/1898/index.html</a>. Accessed 2 August, 2023]
- Sandrik, A., and C. W. Landsea, 2003: Chronological Listing of Tropical Cyclones affecting

  North Florida and Coastal Georgia 1565-1899. NOAA Tech. Memo. NWS SR-224,

  Southern Region, National Weather Service.

- Shutts, G. J., 2005: A kinetic energy backscatter algorithm for use in ensemble prediction systems. *Quart. J. Roy. Meteor. Soc.*, **131**, 3079–3102.
- Slivinski L. C., G. P. Compo, J. S. Whitaker, and Coauthors, 2019: Towards a more reliable historical reanalysis: Improvements for version 3 of the Twentieth Century Reanalysis system. *Q J R Meteorol Soc.* 2019; 145: 2876–2908.https://doi.org/10.1002/qj.3598
- Skamarock W. C., J. B. Klemp, 2008: A time-split nonhydrostatic atmospheric model for weather research and forecasting applications. *Journal of Computational Physics*, 227, Pages 3465-3485, ISSN 0021-9991, <a href="https://doi.org/10.1016/j.jcp.2007.01.037">https://doi.org/10.1016/j.jcp.2007.01.037</a>.
- Smith, R. K., M. T. Montgomery, 2023: *Tropical Cyclones: Observations and Basic Processes* (1<sup>st</sup> edition). Elsevier.
- Sun, Y., Z. Zhong, and W. Lu, 2015: Sensitivity of Tropical Cyclone Feedback on the Intensity of the Western Pacific Subtropical High to Microphysics Schemes. *J. Atmos. Sci.*, **72**, 1346–1368, https://doi.org/10.1175/JAS-D-14-0051.1.
- UGA Extension Forsyth County, 2024: Georgia Agricultural and Forestry Damage from

  Hurricane Helene Estimated at \$6.46 Billion. [Available online at

  <a href="https://site.extension.uga.edu/forsyth/2024/10/georgia-agricultural-and-forestry-damage-from-hurricane-helene-estimated-at-6-46-billion/">https://site.extension.uga.edu/forsyth/2024/10/georgia-agricultural-and-forestry-damage-from-hurricane-helene-estimated-at-6-46-billion/</a>. Accessed 14 April 2025.]

- UCAR, 2023: WRF-ARW Users Guide. [Available online at <a href="https://www2.mmm.ucar.edu/wrf/users/wrf\_users\_guide/build/html/index.html">https://www2.mmm.ucar.edu/wrf/users/wrf\_users\_guide/build/html/index.html</a>. Accessed 26 March 2025]
- U.S. Census Bureau, 1900: 1900 Population States Territories. [Available online at <a href="https://www2.census.gov/library/publications/decennial/1900/bulletins/demographic/20-population-states-territories.pdf">https://www2.census.gov/library/publications/decennial/1900/bulletins/demographic/20-population-states-territories.pdf</a>. Accessed 2 August 2023.]
- U.S. Census Bureau, 2023: County population totals and components of change: 2020-2022.

  [Available online at <a href="https://www.census.gov/data/tables/time-series/demo/popest/2020s-counties-total.html">https://www.census.gov/data/tables/time-series/demo/popest/2020s-counties-total.html</a>. Accessed 2 August 2023.]
- Wang, H., and Y. Wang, 2014: A Numerical Study of Typhoon Megi (2010). Part I: Rapid Intensification. *Mon. Wea. Rev.*, **142**, 29–48, <a href="https://doi.org/10.1175/MWR-D-13-00070.1">https://doi.org/10.1175/MWR-D-13-00070.1</a>.
- Winn, B., J. Bentley, and J. Poudel, 2021: Southern Pulpwood Production, 2021. Southern Research Station Resource Bulletin SRS-257, U.S... Department of Agriculture, Forest Service, 32 pp. [Available online at https://www.srs.fs.usda.gov/pubs/rb/rb\_srs237.pdf, 2 August 2023.]
- Xi, D., N. Lin, and A. Gori, 2023: Increasing sequential tropical cyclone hazards along the US East and Gulf coasts. *Nat. Clim. Chang.*, **13**, 258–265, https://doi.org/10.1038/s41558-023-01595-7.

Zhang, D.-L., and R.A. Anthes, 1982: A high-resolution model of the planetary boundary layer–sensitivity tests and comparisons with SESAME–79 data. *J. Appl. Meteor.*, 21, 1594–1609.